REVIEW

Check for updates

Synthesis and modification of ZIF-8 and its application in drug delivery and tumor therapy

Qiuxiang Wang, Yue Sun, Shangfei Li, Pingping Zhang [ID] * and Qingqiang Yao*

Metal–organic frameworks have the properties of high porosity, variable pore sizes, and easy modification as drug delivery systems. In particular, ZIF-8 based on Zn^{2+} has been extensively studied in the medical field due to its low toxicity and good biocompatibility. This review introduces the preparation and functional modification of ZIF-8, and its application in drug delivery, focusing on the single-stimulus and multi-stimulus response release of drugs in ZIF-8 materials, the integrated role of diagnosis and treatment with ZIF-8 in cancer treatment, and its application in the synergistic therapy of multiple cancer treatment methods. We summarize the latest developments of ZIF-8 in the field of drug delivery and tumor therapy, and present the main challenges that remain to be resolved in the ZIF-8 drug delivery system.

1. Introduction

Coordination polymers are compounds formed by metal ions and inorganic/organic ligands through coordination bonds. Such compounds have been widely studied due to their adjustable structure and diverse functions. A variety of related compounds were synthesized on the basis of coordination polymers, in which metal–organic frameworks (MOFs) are coordination frame materials with a porous structure formed by the coordination of metal ions or metal clusters and organic ligands. MOFs have attracted much attention due to their structural characteristics.

Compared with pure inorganic molecular sieves and porous carbon materials, MOFs have the following advantages: (1) the highly crystalline state of MOFs is very conducive in determining their precise spatial structure with single crystal and polycrystalline diffraction methods; (2) MOFs have high porosity and a specific surface area; (3) MOFs can be composed of various different metal ions and organic bridging ligands, and they have structures that are easy to design; (4) the σ single bond in the organic ligand structure gives MOFs a certain degree of flexibility, so that they have characteristic functions; and (5) the structure is easy to modify: MOFs frame and the structure of the pore surface can be adjusted by modifying the metal center and organic ligands in the MOFs framework so as to give MOFs a variety of functions.

MOFs have shown excellent performance and broad application prospects in adsorption, separation, catalysis, sensing, and drug delivery. In the field of pharmacy, MOFs have attracted much attention because of their high porosity, variable pores, and easily modified features, which give them great application in drug delivery and sustained release.

2. Types of MOFs

Divalent metal ions (especially the first transition series), such as Mn^{2+}, Co^{2+}, Cu^{2+} and Zn^{2+} are often used to build MOFs and are used as drug carriers. According to the soft and hard acid–base theory, these metals have suitable softness and hardness, and the coordination with common donor atoms such as oxygen and nitrogen has moderate coordination reversibility. The reversibility of coordination between divalent metal ions and organic ligands gives the constructed MOFs a unique advantage in drug delivery. When the drug-loaded MOFs carrier is stimulated by a specific pH or heat, the weaker coordination bond is broken and the drug can be released. The monovalent ions such as Cu^+, Ag^+, and K^+ are also commonly used to construct MOFs, but they are so sensitive to light, heat, or water that the stability of the formed MOFs is usually poor, and only by using specific ligands can MOFs with a certain stability be assembled. The coordination bond formed by trivalent metal ions such as Cr^{3+}, Fe^{3+}, Al^{3+} and oxygen-containing ligands (basically carboxylic acids) has larger covalent components, and the formed MOFs often have high chemical and thermal stability. This property makes them easily react with water in the solvent during the synthesis process to form hydroxyl or oxygen-linked poly-nuclear clusters or hydroxides, which hinder the assembly and growth of MOFs. Therefore, the preparation of MOFs with Cr^{3+}, Fe^{3+}, and Al^{3+} as the center often requires acid and very high reaction temperature. Tetravalent metal ions (such as Zr^{4+}) and common oxygen-containing ligands form coordination bonds with more covalent components, and the reaction conditions are more severe.

Institute of Materia Medica, Shandong First Medical University & Shandong Academy of Medical Sciences, Jinan 250062, Shandong, China. E-mail: pingpingzhang6087@163.com; Fax: +86-0531-82919706; Tel: +86-0531-82919706

Table 1 Various MOFs composed of different metal central ions and organic ligands and their applications as drug carriers

MOFs	Metal central ions	Organic ligands	Loaded drug	Applications	Reference
γ-CD-MOFs	K^+	γ-Cyclodextrin (γ-CD)	Fenbufen (FBF)	Analgesic and anti-inflammatory	1
ZIF-8	Zn^{2+}	2-Methylimidazole	5-Fluorouracil (5-fu)	Treatment of colorectal, breast, head and neck cancers	2
ZIF-8	Zn^{2+}	2-Methylimidazole	Doxorubicin (DOX)	Mucoepi-dermoid carcinoma of human lung cells (NCI-H292), human color-ectal adenocarcinoma cells (HT-29) and promyelocytic leukemia cells (HL-60) treatment	3
ZIF-8	Zn^{2+}	2-Methylimidazole	Camptothecin (CPT)	MCF-7 breast cancer cells treatment	4
ZJU-64	Zn^{2+}	[1,1':4',1''-Terphenyl]-4,4''-dicarboxylic acid	Methotrexate (MTX)	Heal acute leukemia	5
Zn-TATAT	Zn^{2+}	5,5'5''-(1,3,5-Triazine-2,4,6-triyl)tris(azanediyl)triisophthalate (TATAT)	5-Fu	Colorectal, breast, and head and neck cancers therapy	6
Bio-MOF-1	Zn^{2+}	Adenine, parabiphenyl-dicarboxylic acid	Procainamide (PROC)	Arrythmia remedy	7
$Zn_2(1,4\text{-bdc})_2(\text{dabco})$	Zn^{2+}	1,4-Benzene dicarboxylate (BDC), 1,4-diazabicyclo [2.2.2] octane(DABCO)	IBU	Analgesic and anti-inflammatory	8
HKUST-1	Cu^{2+}	1,3,5-Benzene tricar-boxylic acid (BTC)	NO	Antithrombotic therapy	9
Fe_3O_4@HKUST-1	Cu^{2+}	BTC	Nimesulid (NIM)	Treatment of pancreatic cancer	10
Fe(bbi)	Fe^{2+}	1,1'-(1,4-Butanediyl)bis(imidazole) (bbi)	DOX·HCl	Heal breast cancer	11
$Mg_2(\text{olz})$	Mg^{2+}	Olsalazine (H_4olz)	Olsalazine (H_4olz)	Ulcerative colitis and colorectal cancer therapy	12
Mn-bisphosphonate@lipid@PEGAA	Mn^{2+}	Zoledronic acid, 1,2-dioleoyl-sn-glycero-3-phosphate sodium salt (DOPA)	Zoledronate	Human breast and pancreatic cancer remedy	13
$[Ni_2(C_8H_2O_6)(H_2O)_2]\cdot 8H_2O$	Ni^{2+}	2,5-Dihydroxyterephthalic acid (H_4dhtp)	NO	Antibacterial, antithrombotic, and wound-healing applications	14
$[Co_2(C_8H_2O_6)(H_2O)_2]\cdot 8H_2O$	Co^{2+}	H_4dhtp	NO	Antibacterial, antithrombotic, and wound-healing applications	14
$\{[Co_2(L)(4,4'\text{-Bipy})_2]CH_3CN\}_n$	Co^{2+}	5,5'-(Biphenyl-4,4'-diyl-bis(methylene))bis(oxy)diisophthalic acid (H_4L), 4,4'-bipyridine	5-Fu	Colorectal, breast, and head and neck cancer therapy	15
MIL-53	Cr^{3+}	BDC	Ibuprofen (IBU)	Analgesic and anti-inflammatory	16
MIL-100	Cr^{3+}	BTC	IBU	Analgesic and anti-inflammatory	17
MIL-101	Cr^{3+}	BDC	IBU	Analgesic and anti-inflammatory	17
MIL-53	Fe^{3+}	BDC	IBU	Analgesic and anti-inflammatory	16
MIL-100	Fe^{3+}	BTC	Busulfan (bu)	Treatment of leukemia	18
MIL-100	Fe^{3+}	BTC	Doxorubicin (DOX)	Heal breast cancer	18
MIL-100	Fe^{3+}	BTC	Azidothimidine triphosphate (AZT-TP)	Anti-HIV	18
MIL-100	Fe^{3+}	BTC	Cidofovir (CDV)	Cure viral infections	18
MIL-101-NH$_2$	Fe^{3+}	Amino-terephthalic acid	AZT-TP	Antiretroviral remedy	18
MIL-101-NH$_2$	Fe^{3+}	Amino-terephthalic acid	CDV	Antiviral therapy	18
MIL-101	Fe^{3+}	BDC	Cisplatin prodrug	Treatment of therioma	19
γ-Fe_2O_3@MIL-53	Al^{3+}	BDC	IBU	Analgesic and anti-inflammatory	20
MOF-In1	In^{3+}	Tris-(para-carboxylphenyl)phosphine oxide (H_3TPO)	5-Fu	Heal colorectal, breast, and head and neck cancers	21

Table 1 (*Contd.*)

MOFs	Metal central ions	Organic ligands	Loaded drug	Applications	Reference
UiONMOF	Zr^{4+}	Aminotriphenyldicarboxylic acid (amino-TPDC)	Cisplatin prodrug, siRNA	Treatment of ovarian cancer	22
UiO-66	Zr^{4+}	BDC	Alendronate (AL)	Extra-skeletal malignancies remedy	23
UiO-66	Zr^{4+}	BDC	Brimonidine tartrate	Chronic glaucoma therapy	24
UiO-67	Zr^{4+}	4,4'-Biphenyldicarboxylic acid (BDPC)	Brimonidine tartrate	Chronic glaucoma therapy	24
Fe_3O_4@UiO-66	Zr^{4+}	BDC	DOX	Cure breast cancer	25
UiO-66-PNIPAM	Zr^{4+}	2-Amino-benzenedicarboxylic acid (H_2N-H_2BDC)	Procainamide (PROC)	Arrythmia remedy	26

Taking into account the stability of the coordination bond between metal ions and organic ligands and the designability of organic ligands, carboxylate and pyridine ligands are often used to synthesize MOFs. The bond forming ability between carboxylate and trivalent/tetravalent metal ions is strong, and carboxylate has a negative charge, which can neutralize the positive charge of metal ions and metal clusters, so it improves the porosity and stability of MOFs. But there are many coordination modes of carboxylate, which are not easy to predict and control. The coordination mode of pyridine ligands is simple, but pyridine ligands is uncharged and their coordination ability is weak, while other components are needed to balance the positive charge of the metal ions. Carboxylate and pyridine ligands can be mixed to meet the coordination and charge requirements. In addition to the carboxylate and pyridine ligands, polyazole molecules such as imidazole and pyrazole have the advantages of carboxylate and pyridine ligands because they can remove a proton to form an anionic multi-terminal ligand. They have strong alkalinity and can form a certain intensity of coordination with metal ions, so that the synthetic MOFs have a certain stability and are widely used. MOFs synthesized from common metal central ions and different organic ligands and their applications as drug carriers are shown in the Table 1.

3. Synthesis and modification of MOFs

Commonly synthesis methods of MOF materials include the conventional solution reaction method, hydrothermal (solvothermal) method (including microwave assisted heating), diffusion method, and mechanical grinding.

The conventional solution reaction method refers to the process of directly mixing the metal salt and the organic bridging ligand in a specific solvent (such as water or organic solvent), adjusting the pH value if necessary, stirring or standing in an open system at not too high a temperature (usually below 100 °C), and precipitating the reaction products in the reaction progresses with the temperature decreases or the solvent evaporates.

The hydrothermal method or solvothermal method refers to the direct mixing of the metal salt and organic co-ligand in a specific solvent (water or organic solvent), and then putting it in a closed reactor. The reactants react under the self-generated pressure of the system through heating.

The diffusion method refers to dissolving two reactants in the same or different solvents respectively, and controlling the reaction conditions so that the two fluids containing reactants come into contact with each other through diffusion at the interface or in a specific medium, thereby reacting to form the target product.

Mechanical grinding refers to mixing and grinding the two solid phases of metal compounds and organic bridging ligand through a ball mill, and reacting to produce the target product.

Sometimes it is necessary to modify the synthesized MOFs in order to introduce some needed functional groups to give MOFs

specific properties. Strictly speaking, MOFs' modification refers to the chemical modification of the metal center and organic bridging ligand after removing the easy-leaving end-capping ligand from the metal center, such as oxidation after synthesis, replacing the easy-to-leave end-capping ligand with ligands with strong coordination ability or soaking MOF crystals to realize the exchange of metal ions or organic ligands.

4. MOFs based on Zn^{2+}

When selecting MOFs as drug carriers, the first thing to consider is whether the MOFs carriers are toxic and the magnitude of toxicity. Therefore, it is necessary that the metal ions and organic ligands used to construct drug-carrying MOFs with good biocompatibility. Some metals such as Cr and Ni are highly toxic, and certain metals themselves are essential elements for human life activities, and the content in the human body is relatively high, such as plasma contains about 22 μM iron and tissues contains zinc (180 μM), copper (68 μM) and manganese (180 μM).[27] These non-toxic metal ions should be preferred when MOFs are synthesized for drug carriers. Of them, Zn^{2+} is an endogenous metal ion commonly and extensively used to construct MOFs.

There are various synthetic methods for Zn-MOFs, including the room temperature solution reaction method, solvothermal method, electrodeposition-solvothermal method, and microfluidic synthesis method. Modification of the synthesized Zn-MOFs can improve their drug loading, sustained release, and controlled release performance. Multifunctional Zn-MOFs can also be designed and synthesized according to needs, such as adding imaging agents to realize integration of diagnosis and treatment, or adding photothermal conversion agents to achieve synergistic treatment of chemotherapy and photothermal therapy.

Among various Zn-based MOFs, $Zn_2(bdc)_2(dabco)$ (bdc = 1,4-benzenedicarboxylic acid, dabco = 1,4-diazabicyclo [2.2.2] octane) is a good candidate for drug loading and sustained release. Motakef-Kazemi *et al.* prepared two different sizes of $Zn_2(bdc)_2(dabco)$ using the solvothermal method under the present and absent of modulator acetic acid. In the case of using the modulator, the synthesized $Zn_2(bdc)_2(dabco)$ has a smaller pore size (100 nm) and a higher ibuprofen loading (30%), while the pore size and drug loading of the sample prepared without using modulator were 250 nm and 22%. Because of the weak interactions between the organic part of the framework and the aromatic rings of ibuprofen, a burst effect appeared in the initial stage of drug release. The release rate of ibuprofen after burst release decreased and the release could prolonged for 3 weeks for the sample with 100 nm pore size.[28] Ma *et al.* synthesized a porous Zn-based MOF $\{[Zn(FDC)]\cdot H_2O\}_n$ (FDC = 2,5-furandicarboxylate) with a (4,8)-connected structure of a rare scu topology. The stability of $\{[Zn(FDC)]\cdot H_2O\}_n$ in water is higher than other MOFs composed of aromatic carboxylates and transition metal ions, and the $\{[Zn(FDC)]\cdot H_2O\}_n$ has high purity. The N_2 adsorption test showed that 5-FU approximately filled up the pores and channels of the $\{[Zn(FDC)]\cdot H_2O\}_n$, showing its high drug loading capacity. The drug release curve

was studied by *in vitro* dialysis, and it was found that there was no "burst effect" within 22 hours. Two distinct stages of the drug release can be observed: 68% (0–22 h) in first stage and 27.6% (22–100 h) in last stage.[29] Luo *et al.* synthesized an unusual nanocage-based framework $[Zn_2(L)(H_2O)_{1.5}]\cdot 5H_2O$ using 2,6-di(3′,5′-dicarboxylphenyl)pyridine as the organic ligand. The prepared framework could be used as a drug carrier to deliver anticancer drug 5-FU, and the maximum drug loading was obtained by adjusting the ratio of the drug to the carrier material. After studying the drug release in neutral and acidic environments, it was found that under acidic conditions, 5-FU could gradually released from the porous framework material in a highly controlled manner.[30] Song *et al.* fabricated a new porous Zn-based MOF $[Zn_3(BTC)_2(Aml)(H_2O)_2](MeOH)_6$ (H_3BTC = 1,3,5-benzenetricarboxylic acid, Aml = ammeline). The nano MOF can be obtained by adding polyvinylpyrrolidone (PVP) in the preparation process. The 5-Fu loaded MOF was prepared in a sealed vessel in the dark with impregnation method. The drug release was found to be 23.9%, 68.6%, 86.5% after being placed in phosphate buffered solution (PBS) for 24 hours under three kinds of pH (7.4, 6.5, and 5.0), demonstrating a pH dependent drug release behavior.[31] By using a strategy of introducing hydrophobic groups to the linkers, Ma *et al.* constructed a new hydrostable Zn-based MOF $[Zn(NO_2\text{-}BDC)(dmbpy)_{0.5}]\cdot(C_2H_6\text{-}O)\cdot(H_2O)$ ($NO_2\text{-}BDC$ = 5-nitroisophthalate, dmbpy = 2,2′-dimethyl- 4,4′-bipyridine, C_2H_6O = ethanol). The drug loading experiment indicated that there was almost no residual porosity after drug adsorption, the busulfan molecules approximately filled up the pores and channels. Busulfan-loaded samples were dispersed in PBS (pH = 7.4), the result shows that the drug release could be divided into two stages: 45% (0–20 h) in the first stage and 55% (20–36 h) in the last stage. The complete release time of busulfan is significantly longer than that of MIL-53 and MIL-100, which might be attributed to the hydrogen-bonding interactions and C–H⋯π stacking interactions involving the busulfan molecules and chemical environment.[32] In terms of antibacterial drug delivery, Duan *et al.* developed a method to coordinate the antibacterial drug pipemidic acid (Hppa) and low-toxic 1,3-benzenedicarboxylate (1,3-bdc) with Zn(II) to build Zn-base MOF $[Zn_2(ppa)_2(1,3\text{-}bdc)(H_2O)]\cdot 2H_2O$ with biological activity, controlled degradation characteristics and interpenetrating structure. The drug release test was conducted in three release media, which were simulated gastric fluid (SGF, 0.01 M HCl solution, pH = 2.0), simulated body fluid (SBF, NaH_2PO_4–Na_2HPO_4 buffer solution pH = 7.4) and simulated intestinum crassum fluid (SIC, $NaHCO_3$ buffer solution pH = 8.3). Regardless of the particle size, the release of Hppa in SGF is the largest, which indicates that the release of Hppa increases with the decrease of pH.[33] Tamames-Tabar *et al.* fabricated a new type of BioMOF (named BioMIL-5) from Zn^{2+} and azelaic acid (AzA) using the hydrothermal method, which has antibacterial and anti-inflammatory properties. The degradation of BioMIL-5 was studied in MilliQ water (simulating skin conditions) and MHCA bacteria broth, and the results showed that the degradation degree of BioMIL-5 in MHCA bacteria broth was much higher than that in MilliQ water. Subsequent experiments proved that BioMIL-5 achieves a bactericidal effect

at a much lower concentration compared with Zn^{2+} and AzA components alone.[34] Xing *et al.* synthesized a bio-friendly Zn-MOF $[Zn(cpon)]_n$, which was constructed by semi-rigid 5-(4'-carboxyphenoxy) nicotinic acid (H_2cpon) under the guidance of the anion template strategy. $[Zn(cpon)]_n$ without any tedious post-synthetic modifications, has showed the prior encapsulating behavior to 5-FU (44.75 wt%) than 6-Mercaptopurine (4.79 wt%), which indicated that the pore size of $[Zn(cpon)]_n$ is more matched with 5-Fu. In addition, under a high temperature environment caused by hyperthermia, the interaction between the drug and the skeleton is destroyed, which can accelerate the drug release rate. The acidic environment will weaken the framework's restriction on 5-Fu, so the drug release speed increases with the pH decreases. Therefore, $[Zn(cpon)]_n$ can be used as a drug carrier that is responsive to the thermal and pH dual-stimulus.[35] Yang *et al.* first synthesized a Zn-based MOF $[Zn_4O(C_8H_5NO_4)_3$, designated as IRMOF-3] by solvothermal method, and then fabricated the folate-conjugated IRMOF-3 (FA-IRMOF-3) by conjugating the amino groups on IRMOF-3 with the carboxylic groups of folic acid. 5-FU finally loaded on the FA-IRMOF-3 to form 5-FU@FA-IRMOF-3 drug carrier particle by the impregnation method. Cytotoxicity experiments showed that folic acid as the targeting ligand on 5-FU@FA-IRMOF-3 enhanced the particle's affinity for FR-positive KB cells (human oral epidermoid carcinoma cell line) and HeLa cells (human cervical carcinoma cell line).[36]

The zeolite imidazole framework (ZIF) is a metal–organic framework composed of Zn^{2+} and imidazole or its derivatives, which is the most widely used drug carrier in Zn-base MOFs. The most representative ZIF is ZIF-8, which is formed by the coordination of Zn^{2+} and the N atom on the 2-methylimidazole ring. Its features are as follows: high porosity, easy modification, certain thermal and chemical stability, low toxicity, and great biocompatibility. ZIF-8 is acid-sensitive and has a pH-responsive drug release function, so it has an excellent performance in drug-controlled release.

4.1 Synthesis methods of ZIF-8

4.1.1 Room temperature solution reaction method. Soltani *et al.* dissolved $Zn(NO_3)_2 \cdot 6H_2O$ in deionized water, then dissolved 2-methylimidazole in ammonium hydroxide solution, and zinc nitrate solution was added to the 2-methylimidazole solution under stirring conditions to form a gray reaction solution. The mixture became a milky suspension after 1 hour, indicating that NZIF-8 nanoparticles (NZIF-8 NPs) had been formed. The synthesized NZIF-8 NPs have a high loading capacity of gentamicin with a loading rate up to 19%. NZIF-8 NPs loaded with gentamicin can release drugs in response to pH, which is expected to treat infectious diseases caused by *Staphylococcus aureus* and *Escherichia coli*.[37]

4.1.2 Solvothermal method. Gao added $Zn(NO_3)_2 \cdot 6H_2O$ methanol solution A to 2-methylimidazole methanol solution B under ultrasonic conditions at room temperature to make a mixed solution. The product after centrifugation of the mixed solution was ultrasonically dispersed in methanol to make solution C. Then the methanol solution of $Zn(NO_3)_2 \cdot 6H_2O$ was

mixed with solution C, and finally transferred to a 50 mL Teflon-lined stainless steel autoclave. After a solvothermal reaction at 120 °C for 2 h, the product was centrifuged and washed several times, and a hollow ZIF-8 with good crystal structure was obtained after vacuum drying.[38] The prepared hollow ZIF-8 possesses a high loading capacity for the anticancer drug 5-fluorouracil. The 5-fluorouracil loaded ZIF-8 material can easily be encapsulated in folic acid-chitosan-5-hydroxyfluorescein (FA-CHI-5-FAM) polymer material to give the drug cell targeting.

4.1.3 Electrodeposition-solvothermal method. Wu *et al.* firstly prepared novel ZnO/2-methylimidazole (ZnO/2-mim) nanocomposite materials with various morphologies by electrochemical deposition. Then the solid mixture of zinc chloride, 2-methylimidazole, and sodium formate was dissolved in anhydrous methanol by ultrasound, and the ZnO/2-mim nanocomposite was added. The mixed reaction solution was put into a Teflon-lined stainless-steel autoclave, and reacted for 24 hours at 85 °C under solvothermal conditions to synthesize a crack-free and uniform ZIF-8 membrane.[39] The ZnO/2-mim nanocomposite material provides abundant reaction sites for the synthesis of a ZIF-8 membrane which has a large specific surface area and thermal stability, and shows a high adsorption capacity for acidic drugs. It can be used for real-time dynamic monitoring of ibuprofen in patients' urine.

4.1.4 Microfluidic synthesis method. Hu *et al.* injected $Zn(NO_3)_2 \cdot 6H_2O$ methanol solution into the T-junction PDMS microfluidic reactor through inlet A with a peristaltic pump at room temperature. Then, the methanol solution containing 2-methylimidazole was stirred for 30 minutes and then divided into two equal parts, which were injected into a microfluidic reactor with a peristaltic pump through inlets B1 and B2 respectively. The product suspension was continuously collected from the outlet of the PDMS monolithic reactor, and white solid product ZIF-8 nanoparticles were obtained after centrifugation and methanol washing.[40] In the same way, ZIF-8@SiO$_2$ composite nanoparticles with a uniform shape, narrow size distribution, good stability, and great biocompatibility can be continuously prepared under the condition of heating at 50 °C. The traits of strong operability and good versatility make the microfluidic synthesis method widely used in the synthesis of drugs and dye molecules loaded ZIF-8 nanocarriers.

4.2 Drug loaded methods of ZIF-8

Phenomena such as poor drug stability and non-specific targeting often occurs when therapeutic drugs are directly used, resulting in reduced drug efficacy. Increasing the amount of treatment can increase the efficacy of the drug, but it will produce greater side effects.[41] ZIF-8 can be used as an intelligent drug delivery carrier to make up for the shortcomings of free drug use. There are two main strategies for loading drugs into ZIF-8: (1) the impregnation method in which drugs are loaded into the pores of MOFs through capillary force, electrostatic interaction, or coordination reaction; (2) in the growth process of MOFs, the *in situ* encapsulation of functional molecules is achieved through the one-pot method to construct drugs/MOF materials.[41]
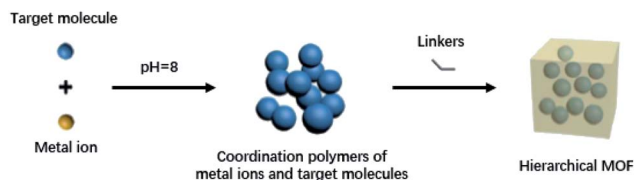
Fig. 1   pH-induced one-pot synthesis of MOF with target molecules.

4.2.1 Impregnation method. Soltani *et al.* used the impregnation method to load the antimicrobial gentamicin (GEN) into nano-ZIF-8 at room temperature to obtain gentamicin@zeolite imidazole framework nanoparticles (GEN@NZIF-8 NPs). They first dissolved GEN in methanol, then added the activated ZIF-8 powder to the GEN methanol solution, and completed the loading GEN into ZIF-8 by stirring at room temperature for 5 days. Finally, the precipitate was collected by centrifugal separation, and GEN@NZIF-8 NPs were obtained by drying after washing the precipitate with methanol.[37]

4.2.2 One-pot method. Zheng *et al.* used a one-pot method to combine the synthesis of ZIF-8 with the anticancer drug DOX packaging process (Fig. 1). They first prepared DOX aqueous solution and 2-methylimidazole (2-mim) aqueous solution, then dissolved $Zn(NO_3)_2 \cdot 6H_2O$ in H_2O to prepare a $Zn(NO_3)_2$ solution (adjusted to pH = 8 by NaOH). The DOX water solution was added to the $Zn(NO_3)_2$ solution, and 2-mim solution was dropped into it after stirring for 1 minute. The reaction mixture was stirred for another 15 minutes, and the precipitate was collected by centrifugation. Finally, the precipitate was washed and dried to obtain DOX@ZIF-8.[42] Kaur *et al.* mixed $Zn(NO_3)_2 \cdot 6H_2O$ aqueous solution, 2-methylimidazole aqueous solution, and 6-mercaptopurine (6-MP) dimethyl sulfoxide solution, which were stirred at room temperature for 5 min. Then, 6-mercaptopurine (used to treat children's acute leukemia and chronic myeloid leukemia) was loaded into ZIF-8 nanoparticles *in situ* using the one-pot method to synthesize 6-MP@ZIF-8 nanomaterials. When 6-MP is loaded into ZIF-8, the shortcomings of 6-MP's poor bioavailability and short plasma half-life are improved, and the drug treatment effect is enhanced.[43] Tiwari *et al.* mixed the $Zn(NO_3)_2 \cdot 6H_2O$ aqueous solution with a methanol solution of 2-methylimidazole and curcumin, which were stirred at room temperature for a certain period of time. Then a curcumin (CCM) encapsulated ZIF-8 nanomaterial (CCM-ZIF-8) was prepared by a one-pot method, and the reaction solution changed from colorless to orange, marking the successful preparation of the drug carrier. ZIF-8, as a delivery vehicle for CCM that is poorly water-soluble and rapidly degrades under physiological conditions, has a high drug load (about 83.33%), and can release drugs in response to an acidic environment.[44]

4.3 Functional modification of ZIF-8

ZIF-8, a representative Zn-MOF drug delivery carrier, is stable under physiological conditions and easily degrades under acidic conditions. The polymers (such as alginic acid and polyethylene glycol) are often used to modify or decorate their surface functions to improve their stability and biocompatibility.[45–47]

After Liu *et al.* synthesized ZIF-8 by the solution method, bis [2-(methacryloyloxy) ethyl] phosphate (BMAP) was added to the DMF solution in which ZIF-8 nanoparticles were dissolved, and a BMAP modified ZIF-8 nanoparticle solution was obtained after incubation at room temperature for 5 h. Then, azobisisobutyronitrile (AIBN) and monomers (such as acrylic acid, poly(ethylene glycol) diacrylate, and poly(ethylene glycol) methyacrylate) were added to the BMAP-modified ZIF-8 nanoparticle solution, and it was incubated at 65 °C for 10 h to obtain polymer-modified ZIF-8. The polymer as a shielding layer can protect ZIF-8 from PO_4^{3-} or acid decomposition, prevent the leakage of loaded drugs, and improve the stability of ZIF-8 under physiological conditions and the stimulus-responsive release of drugs in cells.[45] Vahed *et al.* ball-milled a mixture of zinc acetate and 2-methylimidazole at room temperature to obtain ZIF-8, and then immersed ZIF-8 in the hypoglycemic drug metformin solution for drug loading. Finally, metformin loaded ZIF-8 was added to an alginate aqueous solution and alginate-modified ZIF-8 (ZIF-8@alginate) was obtained by stirring at room temperature. The surface-modified alginate of ZIF-8 increases its stability in acidic media, so that metformin loaded ZIF-8 can safely pass through the acidic media of the stomach and release the drug in the intestinal tract.[46] Wang *et al.* utilized amino poly (ethylene glycol) (PEG-NH₂) to synthesize DOX-loaded PEG-modified metal framework material DOX@ZIF-8/PEG by using a one-pot method. During the synthesis process, the particle size of ZIF-8 can be controlled by adjusting the molar ratio of PEG-NH₂ to 2-mim, and at the same time, the modification of ZIF-8 can be achieved through coordination. Pure ZIF-8 nanoparticles are easy to agglomerate. The colloidal stability of ZIF-8/PEG nanoparticles in water and cell culture fluid is greatly improved after being modified by PEG, and ZIF-8/PEG nanoparticles also have lower toxicity.[47] Surface modification often blocks the pore size of ZIF-8 and causes its drug loading to decrease. In order to solve this problem, Yan *et al.* proposed a method to synthesize an imidazole zeolite framework with controllable size and surface modification using poly-acrylate sodium salt (PAAS) nanospheres as the soft template. They first synthesized PAAS nanospheres and then mixed the nanospheres with $Zn(NO_3)_2$ methanol solution to obtain PAAS-Zn nanospheres. Then the PAAS-Zn nanospheres

Fig. 2   The process of synthesizing ZIF-8 NMOF nanocomposites using PAAS as a soft template.
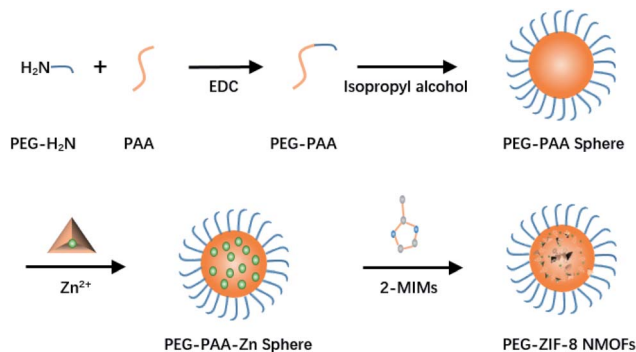
Fig. 3 The process of synthesizing PEG-modified ZIF-8 NMOF nanocomposites using PAAS as a soft template.

Fig. 4 Synthesis process of ZnO-DOX@ZIF-8 nanoparticles and its pH-responsive drug release mechanism.

were dispersed in methanol, and 2-methylimidazole was added into it under stirring (Fig. 2). ZIF-8 of different sizes can be synthesized by controlling the molecular weight of PAAS, and the modified molecule can be coupled with PAAS on the surface of PAAS to achieve surface modification. This method of indirectly modifying the surface of MOFs avoids the problem of low drug loading caused by the decreased porosity of ZIF-8 after modification (Fig. 3).[48] Shearie et al. adopted a ball milling method to improve the hydrophobicity of ZIF-8 by using surface defect strategies. The simple ball milling method with controllable mechanical force can destroy the Zn–N bond on the surface of ZIF-8 and produce unsaturated Zn and N sites, and then the hydrophilicity of ZIF-8 is increased by bonding water molecules in a water environment. This method will not change the structure and size of the internal pores of ZIF-8, and can ensure that the hydrophilic properties of ZIF-8 are improved without affecting its drug loading capacity and release performance.[49]

5. ZIF-8 composite materials

The advantages of a single metal–organic framework for drug delivery are limited. Combining ZIF-8 with other materials (such as mesoporous nanoparticles, proteins, or copolymers) to form composite materials will improve its performance, such as increasing drug loading and biocompatibility, and enhancing the sustained-release effect.

5.1 ZIF-8@Mesoporous nanoparticle composites

ZIF-8 nanoparticles are a good pH-responsive drug delivery vehicle, but the pore size of ZIF-8 nanoparticles is smaller than most drug molecules. Drug molecules are mostly adsorbed on the surface of the particles, resulting in low drug loading.[50] However, mesoporous nanoparticles (such as SiO_2, ZnO, and Fe_3O_4) often possess high drug loading efficiency due to their large specific surface area, and the controlled release of drugs can be achieved by constructing a suitable structure.[50–52] ZIF-8 composite materials can be prepared by combining ZIF-8 with these mesoporous nanoparticles, and the synergistic effect gives them great potential in drug loading, controlled release, and monitoring.
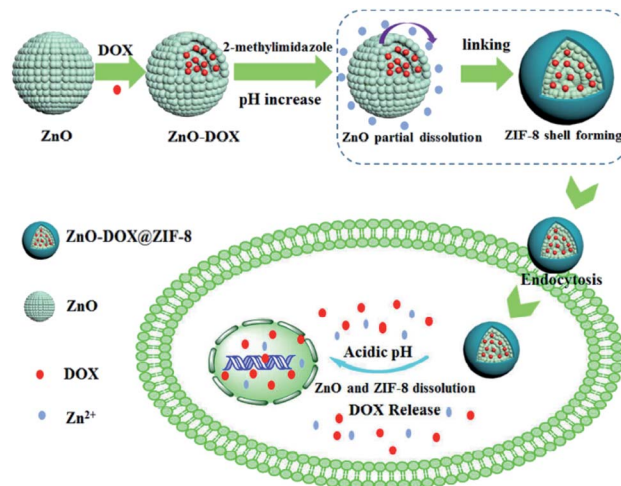
Jia et al. prepared hollow mesoporous silica (HMS) by a two-step method, and then added HMS to DOX ethanol solution to synthesize DOX loaded DOX/HMS. Finally, DOX/HMS was added to the 2-methylimidazole (Hmim) and $Zn(NO_3)_2$ mixed solution and the DOX-loaded silica@zeolite imidazole framework (DOX/HMS@ZIF) was synthesized by stirring at room temperature. The cavity structure and radial channels of HMS are beneficial to the loading and delivery of drugs, and the weight ratio of DOX to HMS can be changed to control the drug loading of DOX. When the weight ratio of DOX to HMS is 1 : 2, the load of DOX can reach 34 wt%, and the load rate is 100%. The capsule structure constructed by DOX/HMS@ZIF encapsulates DOX in the cavity. Under physiological conditions (pH = 7.4), DOX/HMS@ZIF-8 does not release drugs, and only releases drugs at pH = 4–6. In buffer solutions of pH = 6.0, 5.0, and 4.0, the release rates of DOX/HMS@ZIF-8 within 10 h were 46.6%, 71.4%, and 85%, respectively. Compared with free DOX, the DOX/HMS@ZIF-8 drug delivery system has a longer drug release time and a better sustained release effect.[50] Zheng et al. used prefabricated ZnO nanoparticles as a zinc source and coordinated with 2-methylimidazoline ligands to synthesize ZnO-DOX@ZIF-8 nanoparticles with a core/shell structure. ZnO in the core layer is not only a zinc source for the synthesis of MOFs, but also a core to store drugs. The pore size of ZIF-8 shell is smaller than the anti-cancer drug DOX, which protects the drug and avoids the premature release of the drug into the physiological environment. Both ZnO and ZIF-8 are unstable under acidic conditions. When ZnO-DOX@ZIF-8 is internalized by cancer cells, the ZIF-8 shell decomposes under acidic conditions, and the ZnO core is also degraded. The double decomposition of the outer shell and inner core allows the drug to be released for cancer treatment (Fig. 4).[51] Cheng et al. synthesized Fe_3O_4 nanoparticles by the hydrothermal method, then mixed the synthesized Fe_3O_4 nanoparticles with DOX, $Zn(NO_3)_2 \cdot 6H_2O$, 2-methylimidazole, and prepared DOX@Fe_3O_4-ZIF-8 nanocomposite materials by solvothermal reaction. The prepared DOX@Fe_3O_4-ZIF-8 can effectively reduce the activity of liver

cancer cells, promote their apoptosis. The cumulative drug release curve shows that the prepared DOX@Fe_3O_4-ZIF-8 can release DOX slowly and continuously for more than 48 hours. Compared with the burst release phenomenon when using free DOX, DOX@Fe_3O_4-ZIF-8 can achieve continuous treatment of liver cancer. At the same time, the magnetic characteristics of Fe_3O_4 nanoparticles endow DOX@Fe_3O_4-ZIF-8 materials with MRI detection and magnetic separation properties.[52]

5.2 ZIF-8@protein composite material

The composite material composed of ZIF-8 and protein can improve the biocompatibility of ZIF-8. Liang et al. loaded DOX with the biocompatible natural bovine serum albumin (BSA) as the core, and used ZIF-8 as the shell to construct BSA/DOX@ZIF-8 core/shell structure composite material with pH responsiveness and good biocompatibility. MTT cytotoxicity experiments show that BSA/DOX@ZIF composite material is non-toxic to normal cells. Compared with pure ZIF-8 nanoparticles, BSA/DOX@ZIF has better biocompatibility.[53]

5.3 ZIF-8 electrospun fiber composite material

Ghaee et al. modified prepared ZIF-8 nanoparticles with ethylenediamine to obtain MZIF-8, and curcumin was loaded into MZIF-8 by impregnation method to obtain drug-loaded CMZIF-8 nanoparticles. Then CMZIF-8 nanoparticles were dispersed into a mixed solution of polyester (PCL) and urethane prepolymer-based hydrophilic surface-modified macromolecules (LSMM) by using ultrasound. Finally, the mixed solution was electrospun to obtain PCL-LSMM-CMZIF-8 composite nanofibers. MZIF-8 particles can improve the mechanical properties and drug loading efficiency of electrospun fibers. Synthetic PCL-LSMM-CMZIF-8 fiber has great application potential in wound dressing.[54]

5.4 ZIF-8@block copolymer composite material

Lei et al. synthesized a poly(ε-caprolactone) chain transfer agent (PCL-CTA), which was mixed with 4-vinylbenzyl chloride, azobisisobutyronitrile, and tetrahydrofuran to synthesize a block copolymer (PCL-b-PVBC), and then PCL-b-q (PVBC/BPy), referred to as BCP, was obtained through the quaternization reaction of PCL-b-PVBC and 4,4-bipyridine. The two block copolymers, PCL$_{70}$-b-PVBC$_{32}$ and PCL$_{70}$-b-PVBC$_{40}$, were prepared by controlling the reaction conditions. After quaternization, spherical micelles BCP$_{32}$ with an average size of about 200 nm and vesicles BCP$_{40}$ with a bilayer structure were obtained. After the BCP was loaded with DOX by the impregnation method, a core/shell structured drug-loaded block copolymer@ZIF-8 nanocomposite (BCP@ZIF-8) was formed by growing ZIF-8 nanocrystals on the surface of the polymer aggregate. The core of the micelle or the inner cavity of the vesicle stores DOX, and the ZIF-8 shell prevents the premature release of the drug in the physiological environment. Under pH stimulation, the drug-loaded BCP@ZIF-8 has a slower drug release behavior than the DOX-loaded polymer aggregates (without the ZIF-8 shell), which is because the drug encapsulated in polymer aggregates can only be released in cancer cells

after ZIF-8 is decomposed. So the ZIF-8 shell can not only reduce premature drug release under physiological conditions, but also prolongs DOX release under pH stimulation.[55]

6. Application of ZIF-8 in drug delivery

6.1 Drug sustained release

Doxorubicin (DOXO) is a commonly used anthracycline anti-tumor drug, but it has severe cumulative dose-dependent cardiotoxicity. Vasconcelos et al. loaded DOXO into ZIF-8 to synthesize DOXO-ZIF-8, with a loading capacity of 0.049 g DOXO/1 g ZIF-8. DOXO-ZIF-8 can realize the sustained release of DOXO, which can last for 30 days. Since DOXO is slowly released in DOXO-ZIF-8, DOXO-ZIF-8 is less toxic to cells.[3]

Due to the participation of organic ligand azoles, the synthesis of ZIF-8 is often accompanied by the formation of amorphous products, which makes the yield of ZIF-8 low and affects its drug loading rate. Therefore, the control of ZIF-8 synthesis conditions is very important.[56] In addition, if the buffer solution that drug-loaded ZIF-8 comes into contact with during use contains inorganic anions that can form complexes with the central ion Zn^{2+} of ZIF-8, its stability is also affected, which also limits its application as a drug sustained-release carrier.[57] Luzuriaga et al. studied the stability of ZIF-8 single crystals in common laboratory buffers (phosphate buffer and bicarbonate buffer), cell culture media, serum, and whole cell culture media, which provides a reference for the choice of buffer for sustained release of drugs in vitro and in vivo.[58] The size of ZIF-8 particles will also affect the drug release process. Research by Velásquez-Hernández et al. showed that the degradation rate of ZIF-8 particles in phosphate buffered saline (PBS) is related to their size. The smaller the size, the faster the degradation rate of ZIF-8 particles and the faster release of the loaded drug. Therefore, the particle size must be considered when synthesizing drug sustained-release ZIF-8-based composite materials.[59] Duan et al. used non-toxic poly-allylamine hydrochloride (PAH) to synthesize DOX-encapsulated ZIF-8 (DOX@Azif-8) with a one-pot method at room temperature. The reaction was fast, the yield was high, and the prepared DOX@Azif-8 size could be precisely controlled (30–150 nm). As a blocking agent, PAH can compete with organic ligands for coordination with zinc ions, control the super-saturation of the reaction, thus regulate the particle size of the synthesized drug-loaded ZIF-8 through the nucleation step. Investigating the difference in cell uptake of DOX@Azif-8 of different sizes, it was found that cell uptake showed a high degree of particle size dependence (60 > 30 > 90 > 130 nm), and the cell uptake rate of DOX@Azif-8 with 60 nm was the highest. Since the action process of DOX@Azif-8 on cancer cells is a comprehensive result of drug carrier cell internalization and drug release, further investigation of drug release performance is needed. The research results show that the small size, especially 30 nm DOX@Azif-8, has faster release kinetics at pH = 5.0 and pH = 7.4. The smaller the particle size, the faster the drug release, and the higher the instantaneous concentration of

Table 2 Stimulus response-controlled release of various drugs in ZIF-8 and its composites

Stimulus response type	Material	Loaded drug	The release amount in neutral environment (pH = 7.4)	The release amount in acidic environment	Application	Reference
pH	ZIF-8	5-Fu	PBS, 1 h – 17%	Acetate buffer, pH = 5.0, 1 h – 45%, 12 h – 85%	Heal colorectal, breast, head and neck cancers	2
	ZIF-8	Model drug fluorescein	PBS, 24 h – 10%	PBS, pH = 6.0, 1 h – 50%		4
	PAA@ZIF-8	DOX	PBS, 60 h – 35.6%	PBS, pH = 5.5, 60 h – 75.9%	Breast cancer cell MCF-7 treatment	54
	RGD@CPT@ZIF-8	Camptothecin (CPT)	PBS, <5%	PBS, pH = 5.0, 24 h – 75%	Cervical cancer therapy	56
	PEG-NH$_2$@As@ZIF-8	As	PBS, 24 h – 7.2%	PBS, pH = 6.0, 24 h – 20.2%	Treatment of solid tumors	58
	As@ZIF-8	As	PBS, 24 h – 15.5%	PBS, pH = 6.0, 24 h – 29.4%	Treatment of solid tumors	58
	PDA-MSN@ZIF-8	CUR + DOX	PBS, 32 h – 30% CUR + 14% DOX	Acetate buffer, pH = 5.0, 32 h – 86% CUR + 40% DOX	Breast cancer cell MCF-7 treatment	61
	ZIF-8	PHY	PBS, 72 h – 27.61%	PBS, pH = 5.0, 72 h – 88.72%; PBS, pH = 5.4, 72 h – 81.31%	Anti-microbial remedy	62
	Fe$_3$O$_4$@PAA@ZIF-8	Ciprofloxacin (CIP)	PBS, 24 h – 74%	Acetate buffer, pH = 5.0, 2 h – 20%, 3 h – 64%	Heal skin, bone, joint and respiratory infections	63
Targeting	UCNP@ZIF-8/FA	5-Fu	PBS, 12 h – 35%, 24 h – 41.5%	PBS, pH = 5.5, 12 h – 71%, 24 h – 82%	HeLa cells treatment	64
	PEG-FA/PEGCG@ZIF-8	PEGCG	PBS, 48 h <15%	PBS, pH = 6.0, 10 h – 90%	Cervical cancer therapy	65
	CCM@ZIF-8/HA	CCM	PBS, 1 week – 24%	PBS, pH = 5.5, 4 days > 80%	Cervical cancer therapy	66
	HA/α-TOS@ZIF-8	α-TOS	PBS, 25 h – no discernible release	PBS, pH = 5.0, 25 h – 74.0%	HeLa cells treatment	67
Magnetic	Fe$_3$O$_4$@ZIF-8	DOX	PBS, 48 h – 32.6%	PBS, pH = 5.5, 48 h – 63%	Heal breast cancer	70
Light	ZIF-8-TNT	DOX	PBS, the full release of DOX in the presence of UV irradiation: 25 °C – 120 min, 37 °C – 90 min		IMR-32 neuroblastoma remedy	72
pH-redox dual stimulus	DOX@P/ZIF-8	DOX	PBS, in trigger of GSH agents (1×10^{-3} M), 24 h – 21.1%; in trigger of H$_2$O$_2$ agents (1×10^{-3} M), 48 h – 7.0%	Acetate buffer, in trigger of GSH agents (1×10^{-3} M), pH = 5.0 24 h – 81.2%, pH = 4.2 24 h – 100%; in trigger of H$_2$O$_2$ agents (1×10^{-3} M), pH = 5.0 48 h – 79.2%, pH = 4.2 6 h – 100%	Heal human breast cancer	73
pH-light dual stimulus	CoFe$_2$O$_4$@PDA@ZIF-8	CPT + DOX	PBS, without NIR irradiation, 40 h – 13.1% CPT, 3.2% DOX; under an 808 nm NIR laser irradiation(5 min), cumulative release 50.6% CPT, 37.2% DOX	PBS, pH = 5.0, without NIR irradiation, 61.3% CPT, 36.6% DOX; under an 808 nm NIR laser irradiation (5 min), cumulative release 74.8% CPT, 44.6% DOX	Treatment of hepatic carcinoma	75

DOX, the greater the cytotoxicity. Therefore, the anti-cancer ability of DOX@Azif-8 with different particle sizes is: 30 nm > 60 nm > 90 nm > 130 nm.[60]

Stimulus-responsive drug delivery systems are receiving increasing attention because they can receive a stimulus to release a higher concentration of drugs in a specific target site while producing a smaller impact on other parts of the body. Acceptable stimuli include internal variables (pH and glutathione (GSH)) and external stimuli (light, heat, and magnetic field). The stimulus response-controlled release of various drugs in ZIF-8 and their composite materials are list in Table 2.

6.2 Single stimulus response-controlled release of drugs

6.2.1 pH response-controlled release. ZIF-8 can be used as pH-responsive drug release system of anti-cancer drugs, antibacterial drugs, and small molecules. The reason why ZIF-8 is pH sensitive is that acidic conditions can protonate organic ligands, leading to the cleavage of the Zn^+-imidazolium ion coordination bond, thereby decomposing the ZIF-8 skeleton to release the drug.[61,62]

In terms of anti-cancer drug delivery, Sun et al. compared the dissolution characteristics of ZIF-8 in phosphate buffer solution (PBS, pH = 7.4) and acetate buffer solution (pH = 5.0) and found that ZIF-8 dissolves fast under acidic conditions. The pH value of the tumor tissue is between 5.5–6.0, and ZIF-8 is used as the delivery carrier of 5-Fu. In vitro experiments showed that 5-Fu-loaded ZIF-8 has a faster drug release rate in acetate buffer, and can release more than 85% within 12 hours, which is significantly higher than its release rate in neutral solution.[2] Ren et al. used polyacrylate sodium salt nanoparticles (PAAS) as a template to synthesize PAA@ZIF-8 composite material for loading DOX. In vitro experiments showed that the drug release rate of the composite material can reach 75.9% after 60 h under the condition of pH = 5.5, which is much higher than its release in the medium of pH = 7.4.[63] Adhikari et al. compared the drug release rules of ZIF-7 and ZIF-8 as DOX delivery systems at pH = 7.4, 6, 5, and 4. The study found that ZIF-8 is stable under neutral conditions and easily releases drugs under acidic conditions because of the dissociation of metal ions and ligands in the framework in an acidic environment, while ZIF-7 does not release drugs under these four pH values.[64] Dong et al. used ZIF-8 as the carrier of the hydrophobic anticancer drug camptothecin (CPT) to synthesize CPT@ZIF-8 nanoparticles, and then mixed CPT@ZIF-8 nanoparticles with Arg–Gly–Asp (RGD) to construct a CPT-loaded RGD-modified camptothecin@zeolite imidazole framework (RGD@CPT@ZIF-8). In vitro drug release studies have shown that under physiological conditions (pH = 7.4), only a small amount of CPT is released (<5%), but under acidic conditions (PBS, pH = 5.0) for 24 hours, the drug release amount can reach 75%.[65] Arsenic trioxide (ATO) has not been introduced into the treatment of solid tumors due to its dose-limiting toxicity, but in vivo and in vitro studies have shown that it is a potent agent for the treatment of solid tumors. In order to improve its therapeutic effect and reduce its toxic side effects, MOFs can be used as the carrier materials.[66] Ettlinger et al. prepared arsenic loaded As@ZIF-8 nanoparticles

and then modified their surface with amino-functionalized polyethylene glycol derivatives (PEG-NH₂) to obtain PEG-NH₂@As@ZIF-8, which can improve the biocompatibility and stability of As@ZIF-8. In vitro release experiments revealed that under the condition of pH = 7.4, the release amount of arsenic in As@ZIF-8 and PEG-NH₂@As@ZIF-8 after 24 h was 15.5% and 7.2%, respectively, and under the condition of pH = 6, the release of arsenic in 24 h was 29.4% and 20.2%, respectively. This shows that PEG-NH₂@As@ZIF-8 can retain the drug inside the pores under normal tissue conditions (pH = 7.4) and thus protect the environment from the drug toxic side effects, but in the more acidic microenvironment of cancer tissues, the drug can be quickly released to exert its effect. Cytotoxicity experiments show that both As@ZIF-8 and PEG-NH₂@As@ZIF-8 nanoparticles can trigger specific cytotoxicity in rhabdoid tumor cell lines at low concentrations, which is conducive to low-dose tumor treatment. The low therapeutic dose will avoid the possible toxicity of ZIF-8 to non-tumor cells (such as fibroblasts) when applied in vivo.[67] When chemotherapy is used to treat cancer, drug resistance is an important factor that hinders the effectiveness of drugs.[68] Combination medication is an effective way to block drug resistance.[69] Wang et al. synthesized a dopamine-silica@ZIF-8 (PDA-MSN@ZIF-8) core/shell structured nano-carrier to co-deliver DOX and curcumin (CUR). In the drug-loaded PDA-MSN@ZIF-8 system, the CUR-loaded ZIF-8 shell is decomposed in the acidic environment of the tumor to cause the burst release effect of CUR; then the chemotherapeutic drug DOX is continuously released from the core (PDA-MSN) to implement sequential delivery, which can effectively reduce the occurrence of drug resistance (Fig. 5).[70]

In terms of antibacterial drug delivery, Soomro et al. loaded physcion (PHY) with anti-inflammatory and anti-microbial properties into ZIF-8 through a one-pot method at room temperature, which improved the shortcomings of low hydrophilicity and poor bio-compatibility of the drug. The release behavior of PHY@ZIF-8 in PBS (pH = 5.0, 5.4, 7.4) solution was investigated, and the results showed that the cumulative release rate of PHY under acidic conditions (pH = 5.0, 5.4) and a physiological environment (pH = 7.4) after 72 h was 88.72%, 81.31%, and 27.61%, respectively.[71] Ciprofloxacin (CIP) is a fluoroquinolone antibiotic that can be used to treat skin infections, bone and joint infections, and respiratory infections. Esfahanian et al. synthesized Fe_3O_4@poly-acrylic acid (Fe_3O_4@PAA) particles, and then mixed them with $Zn(NO_3)_2 \cdot 6H_2O$ and 2-methylimidazole ethanol solution to prepare Fe_3O_4@PAA@ZIF-8 composite material. Finally, CIP was loaded by the impregnation method to obtain Fe_3O_4@PAA@ZIF-8@CIP drug loaded material. Studies have shown that under the condition of pH = 7.4, the drug releases about 74% after 24 hours and then remains stable, and under the condition of pH = 5, the drug release percentage after 3 hours is about 64%, which is because of the degradation of the metal–organic framework in acidic medium leads to an accelerated release rate of CIP.[72]

In terms of small molecules delivery, due to the poor physiological stability, non-specific targeting, and low cell membrane permeability of small molecules, a higher dose is generally required to achieve the desired therapeutic effect.
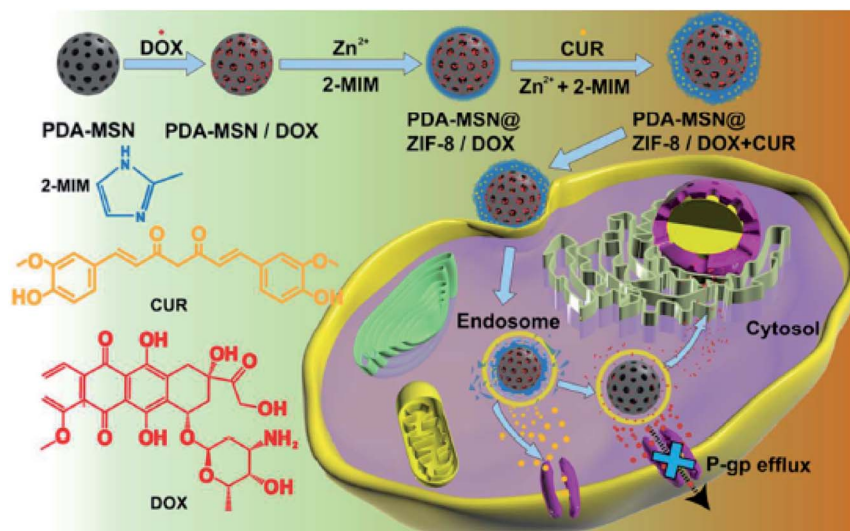
Fig. 5 The synthesis process and drug release mechanism of DOX and CUR loaded PDA-MSN@ZIF-8 core/shell nano-carriers.
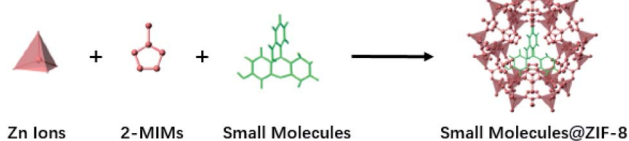

Fig. 6 The process of encapsulating small molecules into ZIF-8.

However, higher dosages will increase drug tolerance and produce adverse side effects. A more ideal therapeutic effect can be achieved by controlling the pH to regulate the release of small molecules. Zhuang *et al.* encapsulated the drug mimic fluorescein into ZIF-8 and synthesized 70 nm-sized drug-loaded nanospheres (the optimal particle size for cell uptake (<100 nm)) (Fig. 6). During the synthesis process, the concentration of fluorescein in the solution can be adjusted to reach different encapsulation amounts. The ZIF-8 nanospheres were immersed in pH = 7.4 and pH = 6.0 PBS respectively. One day later, it was found that the shape and size of the ZIF-8 nanospheres remained unchanged in the pH = 7.4 solution, while the nanospheres disintegrated in the pH = 6.0 solution. In a solution of pH = 7.4, the fluorescein release of ZIF-8 nanospheres in one day was less than 10%, and under the condition of pH = 6.0, the fluorescein release of ZIF-8 nanospheres in one hour reached 50%. This indicates that ZIF-8 can selectively release small-molecule drugs in an acidic environment, thereby realizing controlled release of drugs.[4]

6.2.2 Ligand-receptor targeted localization-controlled release. Folic acid (FA) is a simple and effective active targeting ligand. The folate receptor (FR) is an over-expressed single-chain glycoprotein, which is over-expressed in many malignant tumor cells and thus can be targeted by drug delivery vehicles with folic acid. Conjugating ZIF-8 with an active targeting ligand can deliver the drug to the target site and reduce damage to normal tissues and cells. Chowdhuri *et al.* mixed the three-

component solution containing YCl_3, $YbCl_3$, and $ErCl_3$ with the two-component solution of sodium hydroxide and ammonium fluoride, and synthesized $NaYF_4$:Yb^{3+}, Er^{3+} up-conversion nanoparticles (UCNPs) by the co-precipitation method. Then a core–shell structured nanoparticle (UCNP@ZIF-8/FA) based on UCNPs, MOFs, and FA was constructed by the one-pot method. Finally, the model drug 5-fluorouracil (5-FU) was loaded into it. The core–shell structured drug-loaded particles have pH response and targeted drug delivery capabilities. *In vitro* release experiments showed that after 12 h and 24 h, the release rates of 5-FU in UCNP@ZIF-8/FA under the condition of pH = 7.4 were 35% and 41.5% respectively, while the release rates at pH = 5.5 were 71% and 82% respectively. Fluorescent microscopy studies have found that due to folate receptor-mediated endocytosis, more UCNP@ZIF-8/FA nanoparticles are internalized by cancer cells over time, while the internalization of UCNP@ZIF-8 nanocomposites (without FA) in cancer cells is relatively little.[73] Gao *et al.* synthesized hollow ZIF-8 particles by the solvothermal method, then prepared the FA-CHI-5-FAM copolymer, which was formed by the reaction between the carboxyl group of FA, 5-carboxyfluorescein (5-FAM) and the amino group of the chitosan (CHI) chain. Finally, ZIF-8 particles, the FA-CHI-5-FAM copolymer, and 5-FU were mixed under ultrasound to construct ZIF-8/5-FU@FA-CHI-5-FAM drug delivery microspheres. Among them, FA is an active targeting ligand that can target the drug to a specific location, and 5-FAM as an imaging agent can track the drug delivery process in cells in real time. The targeting of FA was evaluated by incubating ZIF-8/5-FU@FA-CHI-5-FAM and ZIF-8/5-FU@CHI-5-FAM with FA-positive MGC-803 cells and FA-negative HASMC cells respectively for 2 h. Cell uptake imaging showed that compared to ZIF-8/5-FU@CHI-5-FAM, ZIF-8/5-FU@FA-CHI-5-FAM is more easily taken up by MGC-803 cells, but almost cannot enter HASMC cells. The results demonstrated that ZIF-8/5-FU@FA-CHI-5-FAM can target the drug to the tumor site and achieve targeted sustained release of the drug.[38] Epigallocatechin-3-

gallatea (EGCG) is an important biologically active ingredient with strong antioxidant capacity, anti-inflammatory, and anti-cancer activities. In order to improve its stability, Chen *et al.* synthesized an EGCG derivative, EGCG palmitate (PEGCG), then loaded PEGCG into ZIF-8 nanoparticles and performed FA functional modification to construct the PEG-FA/PEGCG@ZIF-8 drug delivery system. MTT tests showed that PEG-FA/PEGCG@ZIF-8 nanoparticles are less toxic to normal cells, and the FA on its surface can recognize the overexpressed folate receptor of the cancer cells, which can effectively internalize PEG-FA/PEGCG@ZIF-8 into the cancer cells and generate a targeting effect on HeLa cancer cells.[74]

Hyaluronic acid (HA) is a hydrophilic natural polysaccharide with negative charge, which is abundant in the extracellular matrix and possesses good biocompatibility, non-toxicity, and biodegradability. In addition, HA can actively target certain tumor cells and bind to the over-expressed CD44 receptor on the surface of tumor cells.[75,76] Li *et al.* synthesized the ZIF-8/HA (ZIF-8 nanocomposite coated with HA) and loaded curcumin (CCM) to synthesize CCM@ZIF-8/HA for cancer treatment. Hydrophilic HA can recognize and bind to the over-expressed CD44 receptor on tumor cells, giving CCM@ZIF-8/HA active targeting ability. *In vitro* drug release experiments showed that there was no initial burst effect at pH = 7.4, and the drug release was only 24% after one week, while the drug could be quickly released at pH = 5.5, and it could reach more than 80% in 4 days. The cellular internalization of free CCM, CCM@ZIF-8, and CCM@ZIF-8/HA after incubated with HeLa cancer cells was observed with a laser confocal scanning microscope. It was found that the active targeting ability of HA facilitated the uptake of CCM@ZIF-8/HA by HeLa cells, showing the strongest fluorescent signal.[75] Sun *et al.* loaded the anticancer drug D-α-Tocopherol succinate (α-TOS) into ZIF-8, and then coupled HA with ZIF-8 to obtain HA/α-TOS@ZIF-8 nanomaterials. The targeting of HA enables HA/α-TOS@ZIF-8 to be phagocytosed by cancer cells through specific interaction with CD44R. When HA/α-TOS@ZIF-8 reaches the tumor site, the hyaluronidase (HAase) in the tumor microenvironment can decompose the HA outer layer, then the exposed α-TOS@ZIF-8 will rapidly degrade under acidic conditions, releasing the drug α-TOS for tumor treatment.[76]

The galactose derivative (G) has a high affinity for hepatoma cells (HepG2) that over-expressed galactagglutinin, and the galactosylation of drug-loaded ZIF-8 could produce better targeting effects on hepatoma cells.[77] Yang *et al.* first synthesized DOX-loaded ZIF-8 (ZIF-8@DOX) by a one-pot method, and then the water-soluble carboxylated pillar [6] arene (WP6) was used as modifiers. ZIF-8@DOX@WP6 was obtained through the coordination of the carboxyl groups on WP6 with the metal nodes on ZIF-8@DOX, which enhanced the water dispersion of ZIF-8@DOX. Then G and ZIF-8@DOX@WP6 were assembled to generate ZIF-8@DOX@WP6@G through the host–guest interaction of WP6 and G. The targeting function of G can improve the targeting ability of the drug delivery carrier to HepG2, so that ZIF-8@DOX@WP6@G has good selectivity and better ability to kill hepatoma cells compared with free DOX.[78]

6.2.3 Magnetic response-controlled release. A porous carrier with fast magnetic response can deliver drugs to specific tissues or organs under the action of a magnetic field, and control the release of drugs through the magnetic response, thereby increasing the effective drug concentration at the target site and reducing the toxic and side effects on normal tissues. ZIF-8 has the advantages of a large pore size range and easy adjustment of pore size. It can be combined with magnetic materials to prepare magnetic ZIF-8 material for the magnetic response controlled-release of drugs.[20]

The magnetic response MOFs drug controlled release system has attracted much attention.[20] Chen *et al.* used sodium acetate and sodium citrate as stabilizers to synthesize Fe_3O_4@ZIF-8 nanoparticles with a core/shell structure in a one-pot method under solvothermal conditions. The DOX loading rate of the prepared Fe_3O_4@ZIF-8 nanoparticles can be as high as 76.6%. Fe_3O_4@ZIF-8 magnetic targeting photothermal effect studies showed that cancer cells in the Fe_3O_4@ZIF-8 enrichment area can be effectively killed after 808 nm laser irradiation, but the effect on cancer cells lacking Fe_3O_4@ZIF-8 is negligible, which indicates that Fe_3O_4@ZIF-8 has obvious magnetic targeting properties.[79]

6.2.4 Thermal response-controlled release. Thermal response-controlled release refers to a method in which a temperature difference between diseased and normal tissues is generated by applying high temperature through an external thermal field, so that a temperature-responsive drug delivery system can release drugs at the diseased tissue.[5]

Silva *et al.* synthesized an adsorbent-heater-thermometer drug-loaded nanomaterial (ZIF-8, EuxTby)@AuNP, which was based on ZIF-8, and the loading and thermal response-controlled release properties of the model drug 5-FU were studied with (ZIF-8, Tb_{20})@AuNP as a typical product. The Au nanoparticles (AuNP) inner core act as controllable nano heater, increasing the temperature of the ZIF-8 shell loaded with 5-FU and triggering the thermal response. The trivalent terbium ion (Tb^{3+}) is doped or adsorbed into ZIF-8, and the outer layer makes use of the special photoluminescent characteristics of Tb^{3+} to construct a molecular thermometer to monitor the temperature in order to ensure that the temperature rise does not damage normal tissues. By studying the thermal controlled-release behavior of (ZIF-8, Tb_{20})@AuNP/5-FU drug carrier system under three different conditions: 514.5 nm irradiation, 50 °C water bath, and room temperature, it was found that: (ZIF-8, Tb_{20})@AuNP/5-FU releases up to 5.7 wt% of the drug in 300 s at room temperature, and the drug release increases to 7 wt% when placed in a water bath at 50 °C for 300 s, while the release amount of the drug reaches 9.7% when irradiated for 300 s, so the use of photothermal conduction can better control the rate and amount of drug release.[80]

6.2.5 Light response-controlled release. Combining ZIF-8 with a semiconductor photocatalyst can prepare a light-responsive drug controlled release system, where the semiconductor photocatalyst will induce the system to generate a local pH gradient under the action of external light (the energy of irradiated photons is higher than the semiconductor band gap), so as to control the drug release.[81]

Sharsheeva *et al.* firstly prepared TiO$_2$ photocatalytic nanotubes (TNTs), and then the TNTs samples were immersed in a Zn(OAc)$_2$·2H$_2$O and 2-methylimidazole solution at room temperature to obtain ZIF-8-TNT particles. Finally, DOXO was loaded into ZIF-8-TNT by the impregnation method to obtain DOXO-ZIF-8-TNT material. The *in vitro* drug release experiments showed that the time required for the complete release of drug from DOXO-ZIF-8-TNT was 41 days and 29 days when the buffer solution of pH = 7.4 was 25 °C and 37 °C, respectively, without UV light irradiation. The release process of the drug can be accelerated after lighting, and the drug can be completely released within 120 min and 90 min, respectively. Using IMR-32 neuroblastoma cells as a model, the drug release amount of DOXO-ZIF-8-TNT was about 50% after 40 minutes of ultraviolet irradiation.[81]

6.3 Dual stimulus response-controlled release of drugs

6.3.1 pH-redox response-controlled release. Compared with normal tissues, the tumor site is an acidic environment, and cancer cells usually express higher concentration of glutathione (GSH) or H$_2$O$_2$, so drug release can be controlled by pH and redox dual stimulation.[82] Zhou *et al.* Directly encapsulated the DOX into the ABA-type diselenide-containing triblock copolymer (PEG-PUSeSe-PEG) micelles to form DOX@P, which was mixed with 2-methylimidazole, and coordinated with Zn^{2+} to make DOX@P grow a ZIF-8 shell on the surface, and finally a core/shell structure of DOX@P/ZIF-8 drug carrier material was obtained. The *in vitro* release profiles of DOX@P/ZIF-8 under different pH conditions (pH = 7.4, 5.0, and 4.2) showed that when triggered by 1×10^{-3} M GSH, the protective effect of the ZIF-8 shell causes DOX@P/ZIF-8 to release only 21.1% of the

drug in 24 hours in the neutral solution, while the decomposition of the ZIF-8 shell under acidic conditions can accelerate the release of the drug, and the release of the drug in 24 h reaches 81.2% (pH = 5.0) and 100% (pH = 4.2), respectively. When triggered by 1×10^{-3} M H$_2$O$_2$, it also has the same pH response release trend. DOX@P/ZIF-8 also has a redox response drug release performance. In a neutral solution without GSH, DOX releases was only 5.1% after 48 hours, and the release amount in acid buffer solution is 1.6% (pH = 5.0) and 14.5% (pH = 4.2), respectively. In a solution containing a lower concentration of GSH (5×10^{-4} M), the release amount of DOX was significantly increased. In a neutral solution, the release amount was nearly 30.5% after 48 h, and the release amount in an acid buffer solution was 43.8% (pH = 5.0) and 100% (pH = 4.2), respectively. In addition, DOX@P/ZIF-8 also has a redox response to H$_2$O$_2$. The acidic condition of the tumor cause the ZIF-8 shell disintegrate, and the structure collapse of ZIF-8 lead to the breakage of the diselenium bond, which can be oxidized to selenate by H$_2$O$_2$ or reduced to selenol by GSH, causing the drug to be released from the PEG-PUSeSe-PEG micelles. This indicates that the DOX@P/ZIF-8 core/shell structure can respond to the slight redox/pH difference between tumor and normal tissues, so as to achieve the controlled-release of DOX under the dual stimulus of pH and redox.[82] Ren *et al.* used a one-pot method to prepare DOX-loaded ZIF-8 (ZDNPs), which was used as the core. The redox-responsive silicone shell containing disulfide bonds was coated on ZDNPs to construct core–shell structured nanoparticles (ZDOS NPs), which were pH and redox dual-stimulus response. ZDOS NPs can remain stable under physiological conditions, and accumulate at the tumor site through the tumor's high permeability and retention effect
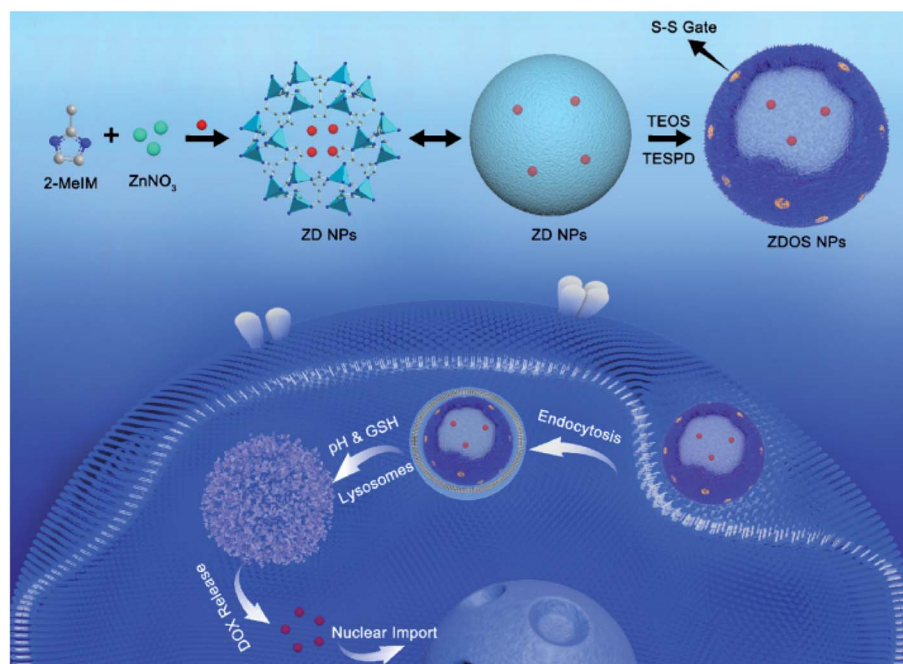

Fig. 7 The preparation and drug release process of ZIF-8@DOX@organosilicon (ZDOS) nanoparticles as a pH and redox dual response drug delivery systems.

(EPR), and are internalized into cancer cells through endocytosis. When encountering endogenous GSH, the disulfide bond of the ZDOS NPs shell will be reduced and ruptured, and the silicone shell will be opened, exposing the ZIF-8 core. ZIF-8 is triggered to dissociate in the acidic tumor microenvironment, which leads to the controlled release of DOX and achieves dual stimulus response to pH and redox (Fig. 7).[83]

6.3.2 pH-light response-controlled release. Near-infrared (NIR) laser is an external light stimulus with active targeting ability. It can control drug delivery "on demand" by adjusting light parameters such as wavelength, intensity, and exposure time. The combination of endogenous pH stimulation and exogenous laser stimulation can achieve the controlled release of drugs under pH-light response dual stimulus.[84]

Yang et al. synthesized a mesoporous $CoFe_2O_4$@PDA@ZIF-8 (CoPZ) sandwich nanocomposite that was pH-NIR dual stimulus response, and two anticancer drugs, the hydrophilic drug doxorubicin (DOX) and the hydrophobic drug camptothecin (CPT) were loaded in $CoFe_2O_4$ and ZIF-8, respectively. The dopamine layer (PDA) interlayer improves the photothermal efficiency and prevents the premature leakage of DOX before it reaches the tumor site. Under pH or NIR stimulation, hydrophilic DOX and hydrophobic CPT exhibit two completely different release behaviors. CoPZ exhibits a continuous drug release process under acidic conditions (pH = 5.0). The rupture of the ZIF-8 shell causes the hydrophobic CPT to be released first, and it reaches a plateau after 12 hours, then hydrophilic DOX embedded in the interior is released. NIR stimulation promotes the simultaneous burst release of CPT and DOX. Under laser irradiation, the $CoFe_2O_4$ core and PDA layer have higher heat transfer capabilities than the ZIF-8 shell, which makes the heat distribution in the nano-carrier uneven. The thermal expansion of CoP is used as a hot spot to crack the nanocarrier from the inside and accelerate the disintegration of the ZIF-8 shell layer and PDA layer, thereby increasing the diffusion rate of CPT and DOX. Two different drug release behaviors enable CoPZ to provide multiple treatment modes of multi-drug chemotherapy, which minimize the side effects of traditional chemotherapy and improves the treatment effect.[84]

7. Application of ZIF-8 in cancer treatment

7.1 Integrated application of tumor diagnosis and treatment

ZIF-8 has the advantages of high porosity, high drug loading rate, and pH response drug controlled release ability. Combining ZIF-8 with imaging technology produces a multifunctional nanocomposite material for integrated diagnosis and treatment of cancer.[85]

He et al. synthesized fluorescent carbon nano-quantum dots, which were combined with ZIF-8 to prepare green fluorescent C-dots@ZIF-8 nanoparticles, and then the anticancer drug 5-Fu was loaded on them. This drug-carrying composite material can realize fluorescent imaging of cancer cells while delivering anticancer drugs, achieving precise treatment.[86] Due to the limited

penetration of fluorescent imaging (FL) and low sensitivity of magnetic resonance imaging (MRI), Qin et al. constructed a new type of multifunctional MOFs material (FZIF-8/DOX-PD-FA). Gd-doped silicon nanoparticles (Si–Gd NPs) were prepared by the hydrothermal method, and then Si–Gd NPs reacted with PVP-K30 to obtain Si–Gd@PVP nanoparticles. In the ZIF-8 synthesis process, Si–Gd@PVP nanoparticles and photosensitizer chlorine e6 (Ce6) were incorporated to obtain FZIF-8 with fluorescent properties, and then DOX was loaded into FZIF-8 by dipping to obtain FZIF-8/DOX. FZIF-8/DOX was modified with preformed pH-responsive polymer poly(2-diethylamino) ethyl methacrylate (HOOC-PDMAEMA-SH) to obtain FZIF-8/DOX-PD. Finally, further surface treatment was performed to obtain a polyethylene glycol-folic acid (PEG-FA) modified composite material FZIF-8/DOX-PD-FA. The Si–Gd nanoparticles and Ce6 in the composite material are used for magnetic resonance and fluorescent imaging, respectively, so that FZIF-8/DOX-PD-FA can be used for precise positioning of tumors to improve the accuracy of diagnosis and treatment. When the photosensitizer Ce6 is irradiated to an excited state by a near-infrared laser, it reacts with oxygen near the tumor cells to generate singlet oxygen (ROS) to kill the tumor cells. Modification of the polymer HOOC-PDMAEMA-SH prevents leakage of the drug during the administration process, then it swells and releases up to 57% DOX under the condition of pH = 6.0 (tumor microenvironment). FZIF-8/DOX-PD-FA has unique dual-mode imaging capabilities and excellent chemical-photodynamic combined treatment effect on cancer, providing a new research platform for expanding the functions of ZIF-8.[87] He et al. prepared porous carbon-coated superparamagnetic Fe_3O_4 nanospheres (Fe_3O_4@C nanospheres) by the solvothermal method, and added them to the methanol solution of $Zn(NO_3)_2 \cdot 6H_2O$ and 2-methylimidazole to induce ZIF-8 growth on the surface of the nanospheres to obtain Fe_3O_4@carbon@ZIF-8 (FCZ) nanoparticles, which were added to DOX-containing PBS (pH = 7.4) to construct DOX loaded DOX@FCZ NPs. The intracellular fluorescent imaging can be performed after embedding carbon quantum dots (CDs) in the porous carbon shell, while superparamagnetic Fe_3O_4 can be used as a T_2^*-weighted magnetic resonance imaging (MRI) contrast agent, so fluorescent and magnetic resonance imaging can diagnose cancer. When DOX@FCZ NPs enter the human body, they are first enriched at the tumor site due to the high permeability and retention effect (EPR) of the tumor. ZIF-8 releases drugs in the acidic environment of acidic endosomes or lysosomal compartments due to its pH sensitivity, thereby accumulating drugs in tumor sites, increasing the local concentration of drugs, and enhancing the therapeutic effect.[88] Bian et al. prepared cetyltrimethylammonium bromide (CTAB) modified monodisperse Fe_3O_4 nanoparticles. Then the Fe_3O_4 nanoparticles aqueous solution, poly-acrylic acid (PAA) aqueous solution and $NH_3 \cdot H_2O$ were ultrasonically mixed, and isopropyl alcohol was dripped into the mixture under magnetic stirring to synthesize Fe_3O_4@PAA core–shell nanoparticles. Prefabricated orange luminescent gold nanoclusters (AuNCs) solution was then added to the Fe_3O_4@PAA core–shell nanoparticle solution. During continuous stirring at room temperature, $Zn(NO_3)_2$ and 2-

methylimidazole (HMeIM) in isopropanol were added into it several times at 30 min intervals to obtain Fe_3O_4@PAA/AuNCs/ZIF-8 composite nanoparticles. Finally, DOX was loaded into Fe_3O_4@PAA/AuNCs/ZIF-8 by dipping. The superparamagnetism of the Fe_3O_4 core in Fe_3O_4@PAA/AuNCs/ZIF-8 composite material makes it is useful as a transverse relaxation (T_2) contrast agent for magnetic resonance imaging (MR). AuNCs have a higher X-ray absorption coefficient than the iodine used in conventional X-ray computed tomography (CT), which makes the CT imaging effect of composite materials better. AuNCs also has photoluminescent properties, and the fluorescent intensity of Fe_3O_4@PAA/AuNCs/ZIF-8 nanoparticles is 2.5 times that of discrete AuNCs, and its fluorescent imaging is better. Multimodal imaging, which combines the three imaging technologies of MR, CT, and optical imaging, can overcome the shortcomings of single imaging. In addition, as the pH decreases, the protonation of the carboxyl group weakens the electrostatic interaction between DOX and PAA, coupled with the pH-sensitive dissolution of ZIF-8, Fe_3O_4@PAA/AuNCs/ZIF-8 nanoparticles have a controlled release of DOX in response to pH.[85] Shu *et al.* prepared DOX@ZIF-8 by loading the chemotherapeutic drug DOX into ZIF-8 by the one-pot method, then polydopamine (PDA) was coated on DOX@ZIF-8 by mussel heuristic polymerization to synthesize DOX@ZIF-PDA. Finally, the hyaluronic acid (HA) was coupled to DOX@ZIF-PDA through the Fe^{3+}-mediated coordination reaction to construct DOX@ZIF-8-HA material. The studies have shown that DOX@ZIF-8-HA has the ability to target prostate cancer cells (PC-3) which is overexpressed CD44. DOX can be quickly released from the carrier material in the acidic tumor environment, increasing the intracellular DOX concentration. In addition, the chelation between Fe^{3+} and PDA gives DOX@ZIF-8-HA good MR imaging capabilities.[89] Au and Ag nanomaterials are often used for surface-enhanced Raman scattering (SERS) imaging. The synergistic effect of bimetals makes the SERS performance of the Au@Ag core/shell nanorod better than that of single metal. However, when loading drugs, the shortcomings of the low specific surface area of Au and Ag limit the loading of drugs. Jiang *et al.* prepared Au nanorods (AuNRS) using a seed-mediated growth method. Then Au@Ag core/shell nanorods (Au@Ag NRS[4-ATP]) were synthesized by the solution reaction method after mixing AuNRS, silver nitrate, and 4-aminothiophenol (4-ATP). 4-ATP gives Au@Ag NRS a strong surface Raman signal. Finally, Au@Ag NRS[4-ATP] reacted with folic acid, $Zn(Ac)_2$, and 2-methylimidazol solution to construct the Au@Ag NRs[4-ATP]@ZIF-8/FA composite carrier. Then the impregnation method was used to load DOX into the composite carrier, which can simultaneously realize SERS imaging and

drug delivery of cancer cells. The ZIF-8 layer of Au@Ag NRs[4-ATP]@ZIF-8/FA allows the metal nanoparticles to avoid the interference of the external environment, thereby making the Raman signal more stable.[90] The bio-imaging systems of near-infrared (NIR) persistent luminescent nanoparticles (PLNPs) can overcome the shortcomings of conventional fluorescent imaging techniques of auto-fluorescent and radiation damage. Lv *et al.* synthesized a chromium-doped zinc gallate@ZIF-8-DOX (ZGGO@ZIF-8-DOX) core/shell structure material, which had the dual functions of near-infrared persistent luminescent imaging and pH-responsive drug delivery (Fig. 8).[91] Zhao *et al.* used the method of surface adsorption-induced self-assembly to grow ZIF-8 *in situ* on the surface of PLNPs ($ZnGa_{1.995}Cr_{0.005}O_4$) to prepare PLNPs@ZIF-8. PLNPs@ZIF-8 shows persistent luminescence activated by acidic tumor sites in tumor imaging. The PLNPs in PLNPs@ZIF-8 can continuously emit near-infrared light for hours or even days without external illumination, which can provide deep tissue penetration and background-free interference imaging. At the same time, the shell layer of the ZIF-8 porous framework provides good drug loading capacity, and successfully achieves drug release triggered by acidic tumor sites.[92]

7.2 Photodynamic therapy

The rapid growth of tumor cells often causes a hypoxic microenvironment (THME) in solid tumors, and the THME will increase the malignancy and metastatic ability of tumors. Photodynamic therapy (PDT) is a method of regulating the THME to treat tumors by increasing the oxygen concentration at the tumor site. Ma *et al.* synthesized ZIF-8 nanoparticles doped with photosensitizer Chlorin e6 (Ce6) and then used the reduction effect of $NaBH_4$ to load nano-Au on the surface of ZIF-8 to prepare Au@ZIF-8. After Au@ZIF-8 reaches the tumor site, nano-Au with catalase-like (CAT) activity decomposes H_2O_2 to generate oxygen, and then converts the oxygen into cytotoxic reactive oxygen species under 660 nm laser irradiation to improve the efficiency of PDT, which provides a simple strategy for cancer treatment *in vivo*.[93]

7.3 Synergistic therapy of tumor by multiple therapies

At present, the traditional treatment methods for malignant tumors mainly include surgical resection, radiotherapy, and chemotherapy, and the new treatment methods involve gene therapy, photothermal therapy, and photodynamic therapy. The complexity of tumor occurrence and development, coupled with the limitations of a single treatment make it difficult for a single treatment method to meet the treatment needs. Multi-modal
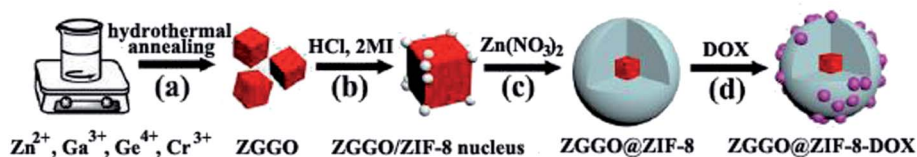

Fig. 8   Preparation of the core–shell structure ZGGO@ZIF-8-DOX multifunctional nano-platform.

synergistic therapy refers to the organic integration of two or more single treatment methods which produces the far greater therapeutic effects. In recent years, ZIF-8 multifunctional composite materials have received extensive attention in the multi-modal synergistic treatment of tumors.[94]

7.3.1 Chemical drug-photothermal combination therapy. Photothermal therapy (PTT) is a minimally invasive local therapy, which uses photothermal conversion agents (such as gold nanoparticles, graphene, ionic liquids, and near-infrared dyes) to generate heat at the tumor site to inhibit the growth of tumors or promote cancer cell apoptosis.[95–97]

Gold nanoparticles have good biocompatibility, high photothermal conversion efficiency, and unique near-infrared (NIR) optical absorption properties.[94] Li et al. coated ZIF-8 on gold nanorods (Au NR) to prepare AuNR@ZIF-8 core/shell nanostructure nanomaterials. The AuNR@ZIF-8 has a larger pore size than that of pure ZIF-8 nanocrystals, which facilitates the loading of larger drug molecules. The AuNR@ZIF-8-DOX composite is obtained by loading DOX into AuNR@ZIF-8 by the impregnation method. The AuNR@ZIF-8-DOX has successfully achieved chemotherapeutic-photothermal tumor combination therapy triggered by near-infrared (NIR) light. The in vivo therapeutic effect of AuNR@ZIF-8-DOX was evaluted by tumor-bearing mice. 4T1 tumor-bearing mice (tumor volume was about 100 mm^3) were randomly divided into 4 groups, then AuNR@ZIF-8 and AuNR@ZIF-8-DOX complexes were injected intravenously into the mice, respectively. The studies showed that mice injected with the AuNR@ZIF-8-DOX complex under near-infrared irradiation had the highest tumor inhibition rate, which was about 90%, while the tumor inhibition rate of mice injected with AuNR@ZIF-8 was about 58% under near-infrared irradiation and the tumor inhibition rate of the AuNR@ZIF-8-DOX complex that did not receive near-infrared radiation was about 30%. This shows that both DOX drug therapy and photothermal therapy play a role in inhibiting tumors, and the combination of chemotherapy and photothermal therapy has the best therapeutic effect, revealing the obvious effective synergy between photothermal therapy and chemotherapy in vivo.[94] The characteristics of low toxicity, easy modification, and good biocompatibility of graphene (GO) make it used for drug delivery, and it has good NIR absorption, high photothermal conversion efficiency, and excellent thermal conductivity, which can be used for photothermal treatment of tumor tissues. Tian et al. mixed the methanol solution of fluorescein (model drug) with 2-methylimidazole and Zn^{2+} solution, then added GO suspension into it to prepare a fluorescein-ZIF-8/GO complex. The release characteristics of fluorescein in buffer solutions with different pH values (pH = 4.5, 6.0 and 7.4) were investigated, and it was found that fluorescein-ZIF-8/GO nanocrystals only released 6% of fluorescein after 10 h in the pH = 7.4 solution. In acidic solution, the release rate of fluorescein-ZIF-8/GO nanocrystals was faster, and the release rate increased with the decrease of pH values. In order to verify the photothermal effect of fluorescein-ZIF-8/GO nanocrystals on cancer cells, 4T1 cells were incubated with 50 and 100 mg ml^{-1} fluorescein-ZIF-8/GO suspensions for 8 hours. Then they were irradiated with an 808 nm laser for 3 min, and 4T1 cells not incubated with

fluorescein-ZIF-8/GO nanocrystals were used as the control group. It was found that when only 4T1 cells were cultured, the presence or absence of laser irradiation had no significant effect on the cell viability. On the contrary, the survival rate of 4T1 cells incubated with fluorescein-ZIF-8/GO suspension was significantly different between 808 nm laser irradiation and non-irradiation. In the two concentrations of fluorescein-ZIF-8/GO suspension without laser irradiation, the cell survival rate was close to 100%, which was attributed to the biocompatibility of fluorescein-ZIF-8/GO nanocrystals. Under laser irradiation, the cell survival rate dropped to about 40% and 21% at the two concentrations of 50 mg ml^{-1} and 100 mg ml^{-1}, respectively. Studies indicated that GO can convert the energy absorbed by NIR into high-capacity heat for the treatment of cancer cells, which shows that the drug-loaded ZIF-8/GO nanocrystals will provide new possibilities for the chemical-photothermal therapy of tumors.[95] Su et al. synthesized ZIF-8/DOX drug-loaded nanoparticles by a one-pot method, and then coated ZrO$_2$ on the surface to obtain ZIF-8/DOX@ZrO$_2$ nanocomposites, which improved the biocompatibility of nano-ZIF-8. Then ionic liquid (IL) was loaded into the pores of the ZIF-8/DOX@ZrO$_2$ nanocomposite by physical methods to construct the ZIF-8/DOX@ZrO$_2$@IL nanocomposite to realize the microwave hyperthermia cancer therapy of the composite material. H22 cells were treated with blank control, free DOX, ZIF-8@ZrO$_2$@IL nanocomposite, and ZIF-8/DOX@ZrO$_2$@IL nanocomposites. It was found that after 7 min of microwave irradiation, the survival rate of each group was 41.4% (blank control group), 23.7% (free DOX), 28.8% (ZIF-8@ZrO$_2$@IL), and 14.6% (ZIF-8/DOX@ZrO$_2$@IL), which indicated that ZIF-8/DOX@ZrO$_2$@IL has a good thermal effect under microwave radiation, and its tumor inhibition rate is significantly higher than other groups. ZIF-8/DOX@ZrO$_2$@IL nanocomposite materials can effectively realize the chemical-microwave synergistic therapy of tumors, and possess a good chemical drug-photothermal synergistic treatment effect on cancer. In addition, since ZrO$_2$ is also an excellent computed tomography (CT) contrast agent, ZIF-8/DOX@ZrO$_2$@IL nanocomposites can also be used to monitor therapy results in real time.[96] When encapsulating drugs in situ during the synthesis of MOFs, only limited drug molecules (such as camptothecin, doxorubicin, caffeine) with special functional groups (–COOH, –SO$_3$H) or opposite charges can successfully interact with MOFs to realize in situ packaging.[97] Zhang et al. proposed a prodrug strategy to solve the problem of drug encapsulation difficulties. Cytarabine (Ara) with poor in situ encapsulation effect was selected as the model drug, and the three-carbocyanine near-infrared dye indocyanine green (IR820) was combined with Ara to form a prodrug (Ara-IR820), and then the Ara-IR820@ZIF-8 material was synthesized with Zn^{2+}, 2-mim and Ara-IR820 by the one-pot method. The sulfonic acid group on IR820 in the prodrug can coordinate with Zn^{2+} in ZIF-8, thereby increasing the drug loading. Finally, the Ara-IR820@ZIF-8 material was modified with hyaluronic acid (HA) to obtain active targeting HA/Ara-IR820@ZIF-8 nanoparticles. The fluorescent imaging of IR820 can be used to diagnose cancer, and the photothermal properties of IR820 can be used for cancer photothermal therapy

(PTT). HA/Ara-IR820@ZIF-8 has a good combined anti-tumor effect of chemotherapy and PTT. Even at low concentrations (10×10^{-6} M) under laser irradiation, the cell inhibition rate of Ara-IR820@ZIF-8 and HA/Ara-IR820@ZIF-8 can reach more than 90%, which is significantly higher than that of IR820 and Ara, and the enhanced cell uptake ability of HA/Ara-IR820@ZIF-8 makes its cell inhibition rate slightly higher than that of Ara-IR820@ZIF-8. The HA/Ara-IR820@ZIF-8 material can remain stable in systemic circulation, and can be trapped into the tumor region by EPR effects and the active targeting of HA. ZIF-8 ruptures under the acidic conditions of the tumor, so that the amide bond in the prodrug Ara-IR820 is hydrolyzed by the overexpressed amidase in the lysosome of the cancer cell, releasing the therapeutic drug Ara. IR820 combined with chemical drugs can achieve excellent tumor targeting and fluorescent imaging guided chemotherapy-photothermal combined therapy.[97]

7.3.2 Chemical drug-photothermal-photodynamic combination therapy. Yang *et al.* added CuS nanoparticles (for photothermal therapy (PTT)), protoporphyrin IX (PpIX) (for PDT), and DOX into the precursor of ZIF-8 through a one-pot method to obtain CuZ@PpIX/DOX. Then the negative cytosine-phosphate-guanine (CpG) was used as an immune adjuvant to be adsorbed on the positive surface of CuZ@PpIX/DOX through electrostatic interaction to inhibit tumor metastasis and recurrence, and dopamine (PDA) was coated on its surface to enhance the PTT effect. At the same time, PDA provides a platform for the growth of MnO_2 and protects the immune activity of CpG, and MnO_2 can be transformed into Mn^{2+} with magnetic resonance imaging activity in the tumor area for T_1-weighted magnetic resonance imaging (MRI). In the final CuZPMn@DOX composite system, the high photothermal conversion efficiency of CuS nanoparticles can trigger the burst release of DOX. PpIX is used for PDT treatment, and chemical drug-photothermal-photodynamic synergistic therapy can effectively eliminate solid tumors. CpG, which has a long-term immune response, can inhibit tumor recurrence and metastasis, and ultimately achieve high efficacy and anti-recurrence/metastatic effects in tumor therapy.[98]

7.3.3 Chemical drug–gene combination therapy. Gene interference (RNAi) can regulate expression of tumor-related proteins, which can inhibit and kill tumor cells. Small interfering RNA (siRNA) is the core of RNAi research. Double-stranded siRNA melts and combines with related proteins in the cytoplasm to form an RNA-induced silencing complex (RISC). The antisense strand of siRNA guides RISC to complementally bind with messenger RNA (mRNA) molecules, and cuts the mRNA at the binding site, which ultimately results in the blocking of the protein translation channel corresponding to the mRNA, leading to the silencing of specific genes. By selectively interfering with and silencing expression of genes involved in tumor production, growth, and spread, tumors can be inhibited or eliminated. Studies have shown that gene silencing not only inhibits tumor cell growth and metastasis, but also inhibits tumor cell resistance to chemotherapeutic drugs. Combining siRNA and chemotherapeutic drugs can effectively enhance tumor treatment effects.[68] Pan *et al.*

ultrasonically treated carboxyl modified mesoporous silica (MSN) and DOX in water, and used the *in situ* growth method to generate ZIF-8 film on the surface of MSN to obtain the DOX-MSN-COOH@ZIF-8 drug system. The positively charged ZIF-8 membrane on the surface of DOX-MSN-COOH@ZIF-8 adsorbs negatively charged Bcl-2 siRNA to obtain a dual delivery system of siRNA and DOX (DOX-MSN-COOH@ZIF-8/Bcl-2 siRNA). The ZIF-8 membrane can encapsulate DOX in MSN pores and protect siRNA from ribonuclease (RNase) degradation. The positively charged ZIF-8 can also promote the uptake of DOX-MSN-COOH@ZIF-8/siRNA by tumor cells and trigger the intracellular release of siRNA and DOX in the acidic tumor environment. Free DOX, DOX-MSN-COOH@ZIF-8, and DOX-MSN-COOH@ZIF-8/Bcl-2 siRNA were incubated with doxorubicin-resistant human breast cancer cells (MCF-7/ADR), respectively. The results of the study showed that compared with the DOX or DOX-MSN-COOH@ZIF-8 system, the vitality of MCF-7/ADR cells significantly decreased in the DOX-MSN-COOH@ZIF-8/Bcl-2 siRNA system that co-delivers DOX and Bcl-2 siRNA. The IC50 values of free DOX, DOX-MSN-COOH@ZIF-8, and DOX-MSN-COOH@ZIF-8/Bcl-2 siRNA on MCF-7/ADR cells were (28.8 ± 0.6), (26.2 ± 0.7), and (9.2 ± 0.4) μM, respectively. These results confirmed that DOX-MSN-COOH@ZIF-8/siRNA nanoparticles co-delivering DOX and siRNA can significantly enhance the therapeutic effect.[68]

7.4 Synthesis of tumor drug-loaded nanocapsules by the ZIF-8 sacrificial template method

Nanocapsules are widely used in the field of controlled drug release because they can improve bioavailability, enhance drug targeting, increase drug stability, and improve drug-controlled release effects. The methods for synthesizing nanocapsules include self-assembly, emulsion polymerization, and the template method. ZIF-8 is a novel template material for synthesizing nanocapsules because it can effectively carry anticancer drugs and can be removed in mild conditions.[99] ZIF-8 has medium strength and stability, and the size and morphology of ZIF-8 can be controlled by adjusting the reaction conditions. Compared with conventional soft and hard templates, ZIF-8 can maintain the uniformity of the template.[100]

Tang *et al.* used synthesized DOX loaded ZIF-8 nanocrystals as a sacrificial template, and the Fe^{3+}-catechol complex was coated on the drug-loaded ZIF-8 nanocrystals through metal ion-organic ligand coordination. Then the ZIF-8 template was removed in a weakly acidic aqueous solution to obtain Fe^{3+}-catechol hollow nanocapsules. The DOX drug molecules remain in the cavity of the hollow nanocapsules, and the coordinated structure of the Fe^{3+}-catechol complex can realize the pH-responsive drug release of the drug-loaded hollow capsules.[99] After encapsulating DOX into ZIF-8 by the co-precipitation method to obtain DOX@ZIF-8, Wang *et al.* added Fe(III) and epigallocatechin-3-gallate (EGCG) aqueous solution to the DOX@ZIF-8 suspension to prepare DOX@ZIF-8 particles with an EGCG/Fe coordination layer. Finally, the ZIF-8 template was removed with EDTA to obtain DOX@EGCG/Fe nanocapsules. ZIF-8 acts as a sacrificial template for the formation of the inner

cavity of the nanocapsules during the preparation process, and EGCG enables the drug-loaded nanocapsules have a reactive oxygen species (ROS) stimulation response drug release performance.[101] Fang *et al.* coated the Au/polydopamine (Au/PDA) on the ZIF-8 by *in situ* polymerization of $HAuCl_4$ and dopamine, while the template was etched to obtain cubic-shaped Au/PDA hybrid microcapsules with adjustable nanostructure. Two different cubic microcapsules, hollow and yolk microcapsules, can be obtained by changing the synthesis kinetics. The Au/PDA cube microcapsules were added to an ibuprofen/*n*-hexane solution at room temperature, and then stirred and centrifuged to obtain the Au/PDA cube drug-loaded microcapsules loaded with the analgesic and anti-inflammatory drug ibuprofen.[102] After Zou *et al.* synthesized ZIF-8 nanocrystals, they used an improved sol–gel method to coat the surface of ZIF-8 nanocrystals with a mesoporous silica layer to form ZIF-8@MSN. Then the ZIF-8 was naturally degraded in dilute hydrochloric acid solution to obtain monodispersed hollow mesoporous silica (HMSN). The prepared HMSN has a huge inner cavity and a narrow pore structure perpendicular to the surface. The anticancer drug DOX was encapsulated, and then ZIF-8 was applied as a pore blocker on the surface of the HMSN to obtain DOX/MSN@ZIF-8, which can successfully construct pH-responsive intracellular administration capsules.[100]

8. Outlook

In recent years, MOFs has attracted more and more attention in the medical field due to their controllable aperture, easy modification, and high drug storage capacity. Among them, ZIF-8 has been extensively studied in the field of drug delivery because of its high porosity, easy modification, and good biocompatibility. This review introduces the preparation process, functional modification methods of ZIF-8, and the latest research progress of ZIF-8 composite materials, and introduces the application of ZIF-8 in drug delivery and tumor therapy in detail. ZIF-8 has pH response characteristics, so it can release high concentrations of drugs after reaching the acidic environment of the tumor. In addition, ZIF-8 can also be designed as other stimulus-responsive drug delivery systems (light, heat, magnetic field, targeted location, GSH, H_2O_2 stimulation, *etc.*) to control the release of drugs at specific sites to reduce the toxic side effect on normal tissue sites. Combining ZIF-8 with imaging technologies (such as fluorescent imaging, nuclear magnetic resonance imaging, and near-infrared persistent luminescent imaging) can expand its functions, and realize the integration of cancer diagnosis and therapy, and greatly improve the accuracy and effectiveness of tumor treatment. A single cancer therapy method has certain limitations. The combination of multiple treatment methods (chemotherapy, photothermal therapy, and photodynamic therapy, *etc*) can improve the therapeutic effect of cancer and minimize the side effects. Composite materials with multiple functions are currently a hot spot in the field of biomedical research. For example, nano-gold and graphene can be composited with ZIF-8 to prepare multifunctional biomaterials.

These multifunctional materials can improve the drug loading, stability, and biocompatibility of ZIF-8 drug delivery system, realizing integrated diagnosis and treatment, and multi-therapy synergistic treatment of cancer. However, there have been few *in vivo* safety assessments of multifunctional composite materials. The poor biodegradability of certain materials under physiological conditions also limits their development to a certain extent. More biodegradable and biocompatible ZIF-8 multifunctional composite materials need to be urgently developed. At present, covalent-metal frame materials (COFs) have attracted wide attention due to their excellent properties such as adjustable structure, high surface area, and good stability. The combination of ZIF-8 and COFs is expected to develop new multifunctional bio-composites. In addition, the drug delivery system of ZIF-8 and its composite materials are mainly administered by injection, and a small amount is implanted for local delivery at the lesion site. The richness of drug delivery forms is also a challenge for the practical application of ZIF-8 materials.

Conflicts of interest

There are no conflicts to declare.

Acknowledgements

References

1 B. T. Liu, Y. P. He, L. P. Han, V. Singh, X. N. Xu, T. Guo, F. Y. Meng, X. Xu, P. York, Z. X. Liu and J. W. Zhang, *Cryst. Growth Des.*, 2017, **17**, 1654–1660.

2 C. Y. Sun, C. Qin, X. L. Wang, G. S. Yang, K. Z. Shao, Y. Q. Lan, Z. M. Su, P. Huang, C. G. Wang and E. B. Wang, *Dalton Trans.*, 2012, **41**, 6906–6909.

3 I. B. Vasconcelos, T. G. da Silva, G. C. G. Militão, T. A. Soares, N. M. Rodrigues, M. O. Rodrigues, N. B. Costa Jr, R. O. Freire and S. A. Junior, *RSC Adv.*, 2012, **2**, 9437–9442.

4 J. Zhuang, C. H. Kuo, L. Y. Chou, D. Y. Liu, E. Weerapana and C. K. Tsung, *ACS Nano*, 2014, **8**, 2812–2819.

5 W. X. Lin, Q. Hu, J. C. Yu, K. Jiang, Y. Y. Yang, S. C. Xiang, Y. J. Cui, Y. Yang, Z. Y. Wang and G. D. Qian, *ChemPlusChem*, 2016, **81**, 804–810.

6 C. Y. Sun, C. Qin, C. G. Wang, Z. M. Su, S. Wang, X. L. Wang, G. S. Yang, K. Z. Shao, Y. Q. Lan and E. B. Wang, *Adv. Mater.*, 2011, **23**, 5629–5632.

7 J. An, S. J. Geib and N. L. Rosi, *J. Am. Chem. Soc.*, 2009, **131**, 8376–8377.

8 N. Motakef-Kazemi, S. A. Shojaosadati and A. Morsali, *Microporous Mesoporous Mater.*, 2014, **186**, 73–79.

9 B. Xiao, P. S. Wheatley, X. B. Zhao, A. J. Fletcher, S. Fox, A. G. Rossi, I. L. Megson, S. Bordiga, L. Regli, K. M. Thomas and R. E. Morris, *J. Am. Chem. Soc.*, 2007, **129**, 1203–1209.

10 F. Ke, Y. P. Yuan, L. G. Qiu, Y. H. Shen, A. J. Xie, J. F. Zhu, X. Y. Tian and L. D. Zhang, *J. Mater. Chem.*, 2011, **21**, 3843–3848.

11 P. F. Gao, L. L. Zheng, L. J. Liang, X. X. Yang, Y. F. Li and C. Z. Huang, *J. Mater. Chem. B*, 2013, **1**, 3202–3208.

12 D. J. Levine, T. Runcevski, M. T. Kapelewski, B. K. Keitz, J. Oktawiec, D. A. Reed, J. A. Mason, H. Z. H. Jiang, K. A. Colwell, C. M. Legendre, S. A. FitzGerald and J. R. Long, *J. Am. Chem. Soc.*, 2016, **138**, 10143–10150.

13 D. M. Liu, C. B. He, C. Poon and W. B. Lin, *J. Mater. Chem. B*, 2014, **2**, 8249–8255.

14 A. C. McKinlay, B. Xiao, D. S. Wragg, P. S. Wheatley, I. L. Megson and R. E. Morris, *J. Am. Chem. Soc.*, 2008, **130**, 10440–10444.

15 F. M. Wang, J. Wang, S. Z. Yang, C. Y. Gu, X. R. Wu, J. Q. Liu, H. Sakiyama, J. W. Xu, M. M. Luo and W. C. Liu, *Russ. J. Coord. Chem.*, 2017, **43**, 133–137.

16 P. Horcajada, C. Serre, G. Maurin, N. A. Ramsahye, F. Balas, M. Vallet-Regí, M. Sebban, F. Taulelle and G. Férey, *J. Am. Chem. Soc.*, 2008, **130**, 6774–6780.

17 P. Horcajada, C. Serre, M. Vallet-Regí, M. Sebban, F. Taulelle and G. Férey, *Angew. Chem., Int. Ed.*, 2006, **45**, 5974–5978.

18 P. Horcajada, T. Chalati, C. Serre, B. Gillet, C. Sebrie, T. Baati, J. F. Eubank, D. Heurtaux, P. Clayette, C. Kreuz, J. S. Chang, Y. K. Hwang, V. Marsaud, P. Bories, L. Cynober, S. Gil, G. Férey, P. Couvreur and R. Gref, *Nat. Mater.*, 2010, **9**, 172–178.

19 K. M. L. Taylor-Pashow, J. D. Rocca, Z. G. Xie, S. Tran and W. B. Lin, *J. Am. Chem. Soc.*, 2009, **131**, 14261–14263.

20 Y. N. Wu, M. M. Zhou, S. Li, Z. H. Li, J. Li, B. Z. Wu, G. T. Li, F. T. Li and X. H. Guan, *Small*, 2014, **10**, 2927–2936.

21 X. Du, R. Q. Fan, L. S. Qiang, K. Xing, H. X. Ye, X. Y. Ran, Y. Song, P. Wang and Y. L. Yang, *ACS Appl. Mater. Interfaces*, 2017, **9**, 28939–28948.

22 C. B. He, K. D. Lu, D. M. Liu and W. B. Lin, *J. Am. Chem. Soc.*, 2014, **136**, 5181–5184.

23 X. Y. Zhu, J. L. Gu, Y. Wang, B. Li, Y. S. Li, W. R. Zhao and J. L. Shi, *Chem. Commun.*, 2014, **50**, 8779–8782.

24 J. Gandara-Loe, I. Ortuño-Lizarán, L. Fernández-Sanchez, J. L. Alio, N. Cuenca, A. V. Estrada and J. Silvestre-Albero, *ACS Appl. Mater. Interfaces*, 2019, **11**, 1924–1931.

25 H. X. Zhao, Q. Zou, S. K. Sun, C. S. Yu, X. J. Zhang, R. J. Li and Y. Y. Fu, *Chem. Sci.*, 2016, **7**, 5294–5301.

26 S. Nagata, K. Kokado and K. Sada, *Chem. Commun.*, 2015, **51**, 8614–8617.

27 R. C. Huxford, J. D. Rocca and W. B. Lin, *Curr. Opin. Chem. Biol.*, 2010, **14**, 262–268.

28 N. Motakef-Kazemi, S. A. Shojaosadati and A. Morsali, *J. Iran. Chem. Soc.*, 2016, **13**, 1205–1212.

29 D. Y. Ma, J. M. Xie, Z. W. Zhu, H. L. Huang, Y. T. Chen, R. X. Su and H. M. Zhu, *Inorg. Chem. Commun.*, 2017, **86**, 128–132.

30 Z. D. Luo, R. Wang, C. Y. Gu, F. M. Li, Y. Y. Han, B. H. Li and J. Q. Liu, *Inorg. Chem. Commun.*, 2017, **76**, 91–94.

31 B. H. Song, X. Ding, Z. F. Zhang and G. F. An, *J. Iran. Chem. Soc.*, 2018, **16**, 333–340.

32 D. Y. Ma, Z. Li, J. X. Xiao, R. Deng, P. F. Lin, R. Q. Chen, Y. Q. Liang, H. F. Guo, B. Liu and J. Q. Liu, *Inorg. Chem.*, 2015, **54**, 6719–6726.

33 L. N. Duan, Q. Q. Dang, C. Y. Han and X. M. Zhang, *Dalton Trans.*, 2015, **44**, 1800–1804.

34 C. Tamames-Tabar, E. Imbuluzqueta, N. Guillou, C. Serre, S. R. Miller, E. Elkaïm, P. Horcajada and M. J. Blanco-Prieto, *CrystEngComm*, 2015, **17**, 456–462.

35 K. Xing, R. Q. Fan, F. Y. Wang, H. Nie, X. Du, S. Gai, P. Wang and Y. L. Yang, *ACS Appl. Mater. Interfaces*, 2018, **10**, 22746–22756.

36 B. C. Yang, M. Shen, J. Q. Liu and F. Ren, *Pharm. Res.*, 2017, **34**, 2440–2450.

37 B. Soltani, H. Nabipour and N. A. Nasab, *J. Inorg. Organomet. Polym. Mater.*, 2017, **28**, 1090–1097.

38 X. C. Gao, X. Hai, H. Baigude, W. H. Guan and Z. L. Liu, *Sci. Rep.*, 2016, **6**, 37705–37714.

39 M. Wu, H. L. Ye, F. Q. Zhao and B. Z. Zeng, *Sci. Rep.*, 2017, **7**, 39778–39786.

40 G. F. Hu, L. L. Yang, Y. N. Li and L. Y. Wang, *J. Mater. Chem. B*, 2018, **6**, 7936–7942.

41 X. R. Chen, R. L. Tong, Z. Q. Shi, B. Yang, H. Liu, S. P. Ding, X. Wang, Q. F. Lei, J. Wu and W. J. Fang, *ACS Appl. Mater. Interfaces*, 2018, **10**, 2328–2337.

42 H. Q. Zheng, Y. N. Zhang, L. F. Liu, W. Wan, P. Guo, A. M. Nyström and X. D. Zou, *J. Am. Chem. Soc.*, 2016, **138**, 962–968.

43 H. Kaur, G. C. Mohanta, V. Gupta, D. Kukkar and S. Tyagi, *J. Drug Deliv. Sci. Technol.*, 2017, **41**, 106–112.

44 A. Tiwari, A. Singh, N. Garg and J. K. Randhawa, *Sci. Rep.*, 2017, **7**, 12598–12609.

45 Y. Liu, C. S. Gong, Y. L. Dai, Z. Yang, G. C. Yu, Y. J. Liu, M. R. Zhang, L. S. Lin, W. Tang, Z. J. Zhou, G. Z. Zhu, J. J. Chen, O. Jacobson, D. O. Kiesewetter, Z. T. Wang and X. Y. Chen, *Biomaterials*, 2019, **218**, 119365–119375.

46 T. A. Vahed, M. R. Naimi-Jamal and L. Panahi, *J. Drug Deliv. Sci. Technol.*, 2019, **49**, 570–576.

47 H. H. Wang, T. Li, J. W. Li, W. J. Tong and C. Y. Gao, *Colloids Surf., A*, 2019, **568**, 224–230.

48 L. Yan, X. F. Chen, Z. G. Wang, X. J. Zhang, X. Y. Zhu, M. J. Zhou, W. Chen, L. B. Huang, V. A. L. Roy, P. K. N. Yu, G. Y. Zhu and W. J. Zhang, *ACS Appl. Mater. Interfaces*, 2017, **9**, 32990–33000.

49 E. Shearier, P. F. Cheng, J. M. Bao, Y. H. Hu and F. Zhao, *RSC Adv.*, 2016, **6**, 4128–4135.

50 X. M. Jia, Z. Y. Yang, Y. J. Wang, Y. Chen, H. T. Yuan, H. Y. Chen, X. X. Xu, X. Q. Gao, Z. Z. Liang, Y. Sun, J. R. Li, H. Q. Zheng and R. Cao, *ChemMedChem*, 2018, **13**, 400–405.

51 C. C. Zheng, Y. Wang, S. Z. F. Phua, W. Q. Lim and Y. L. Zhao, *ACS Biomater. Sci. Eng.*, 2017, **3**, 2223–2229.

52 C. Cheng, C. Li, X. L. Zhu, W. Han, J. H. Li and Y. Lv, *J. Biomater. Appl.*, 2019, **33**, 1373–1381.

53 Z. Z. Liang, Z. Y. Yang, H. T. Yuan, C. Wang, J. Qi, K. Q. Liu, R. Cao and H. Q. Zheng, *Dalton Trans.*, 2018, **47**, 10223–10228.

54 A. Ghaee, M. Karimi, M. Lotfi-Sarvestani, B. Sadatnia and V. Hoseinpour, *Mater. Sci. Eng., C*, 2019, **103**, 109767–109779.

55 Z. T. Lei, Q. J. Tang, Y. S. Ju, Y. H. Lin, X. W. Bai, H. P. Luo and Z. Z. Tong, *J. Biomater. Sci., Polym. Ed.*, 2020, **31**, 695–711.

56 X. L. Liu, Q. Yin, G. Huang and T. F. Liu, *Inorg. Chem. Commun.*, 2018, **94**, 21–26.

57 J. Wang, D. Y. Ma, W. L. Liao, S. J. Li, M. F. Huang, H. M. Liu, Y. F. Wang, R. Xie and J. Xu, *CrystEngComm*, 2017, **19**, 5244–5250.

58 M. A. Luzuriaga, C. E. Benjamin, M. W. Gaertner, H. Lee, F. C. Herbert, S. Mallick and J. J. Gassensmith, *Supramol. Chem.*, 2019, **31**, 485–490.

59 M. de J. Velásquez-Hernández, R. Ricco, F. Carraro, F. T. Limpoco, M. Linares-Moreau, E. Leitner, H. Wiltsche, J. Rattenberger, H. Schröttner, P. Frühwirt, E. M. Stadler, G. Gescheidt, H. Amenitsch, C. J. Doonan and P. Falcaro, *CrystEngComm*, 2019, **21**, 4538–4544.

60 D. B. Duan, H. Liu, M. X. Xu, M. Q. Chen, Y. X. Han, Y. X. Shi and Z. B. Liu, *ACS Appl. Mater. Interfaces*, 2018, **10**, 42165–42174.

61 J. Fang, Y. Yang, W. Xiao, B. W. Zheng, Y. B. Lv, X. L. Liu and J. Ding, *Nanoscale*, 2016, **8**, 3259–3263.

62 Z. Q. Shi, X. R. Chen, L. Zhang, S. P. Ding, X. Wang, Q. F. Lei and W. J. Fang, *Biomater. Sci.*, 2018, **6**, 2582–2590.

63 H. Ren, L. Y. Zhang, J. P. An, T. T. Wang, L. Li, X. Y. Si, L. He, X. T. Wu, C. G. Wang and Z. M. Su, *Chem. Commun.*, 2014, **50**, 1000–1002.

64 C. Adhikari, A. Das and A. Chakraborty, *Mol. Pharmaceutics*, 2015, **12**, 3158–3166.

65 K. Dong, Y. Zhang, L. Zhang, Z. Z. Wang, J. S. Ren and X. G. Qu, *Talanta*, 2019, **194**, 703–708.

66 R. Ettlinger, M. Sönksen, M. Graf, N. Moreno, D. Denysenko, D. Volkmer, K. Kerl and H. Bunzen, *J. Mater. Chem. B*, 2018, **6**, 6481–6489.

67 R. Ettlinger, N. Moreno, D. Volkmer, K. Kerl and H. Bunzen, *Chem.–Eur. J.*, 2019, **25**, 13189–13196.

68 Q. S. Pan, T. T. Chen, C. P. Nie, J. T. Yi, C. Liu, Y. L. Hu and X. Chu, *ACS Appl. Mater. Interfaces*, 2018, **10**, 33070–33077.

69 F. M. Zhang, H. Dong, X. Zhang, X. J. Sun, M. Liu, D. D. Yang, X. Liu and J. Z. Wei, *ACS Appl. Mater. Interfaces*, 2017, **9**, 27332–27337.

70 L. C. Wang, H. D. Guan, Z. Q. Wang, Y. X. Xing, J. X. Zhang and K. Y. Cai, *Mol. Pharmaceutics*, 2018, **15**, 2503–2512.

71 N. A. Soomro, Q. Wu, S. A. Amur, H. Liang, A. Ur Rahman, Q. P. Yuan and Y. Wei, *Colloids Surf., B*, 2019, **182**, 110364–110370.

72 M. Esfahanian, M. A. Ghasemzadeh and S. M. H. Razavian, *Artif. Cells, Nanomed., Biotechnol.*, 2019, **47**, 2024–2030.

73 A. R. Chowdhuri, D. Laha, S. Pal, P. Karmakar and S. K. Sahu, *Dalton Trans.*, 2016, **45**, 18120–18132.

74 X. R. Chen, Z. Q. Shi, R. L. Tong, S. P. Ding, X. Wang, J. Wu, Q. F. Lei and W. J. Fang, *ACS Biomater. Sci. Eng.*, 2018, **4**, 4183–4192.

75 Y. Q. Li, Y. T. Zheng, X. Y. Lai, Y. H. Chu and Y. M. Chen, *RSC Adv.*, 2018, **8**, 23623–23628.

76 Q. Q. Sun, H. T. Bi, Z. Wang, C. X. Li, X. W. Wang, J. T. Xu, H. Zhu, R. X. Zhao, F. He, S. L. Gai and P. P. Yang, *Biomaterials*, 2019, **223**, 119473–119483.

77 W. Chen, Y. Zou, F. H. Meng, R. Cheng, C. Deng, J. Feijen and Z. Y. Zhong, *Biomacromolecules*, 2014, **15**, 900–907.

78 K. Yang, K. Yang, S. Chao, J. Wen, Y. X. Pei and Z. C. Pei, *Chem. Commun.*, 2018, **54**, 9817–9820.

79 G. H. Chen, B. Yu, C. H. Lu, H. H. Zhang, Y. Q. Shen and H. L. Cong, *CrystEngComm*, 2018, **20**, 7486–7491.

80 J. Y. R. Silva, Y. G. Proenza, L. L. da Luz, S. de Sousa Araújo, M. A. G. Filho, S. A. Junior, T. A. Soares and R. L. Longo, *Mater. Sci. Eng., C*, 2019, **102**, 578–588.

81 A. Sharsheeva, V. A. Iglin, P. V. Nesterov, O. A. Kuchur, E. Garifullina, E. Hey-Hawkins, S. A. Ulasevich, E. V. Skorb, A. V. Vinogradov and M. I. Morozov, *J. Mater. Chem. B*, 2019, **7**, 6810–6821.

82 W. Q. Zhou, L. Wang, F. Li, W. N. Zhang, W. Huang, F. W. Huo and H. P. Xu, *Adv. Funct. Mater.*, 2017, **27**, 1605465–1605472.

83 S. Z. Ren, D. Zhu, X. H. Zhu, B. Wang, Y. S. Yang, W. X. Sun, X. M. Wang, P. C. Lv, Z. C. Wang and H. L. Zhu, *ACS Appl. Mater. Interfaces*, 2019, **11**, 20678–20688.

84 J. C. Yang, Y. Chen, Y. H. Li and X. B. Yin, *ACS Appl. Mater. Interfaces*, 2017, **9**, 22278–22288.

85 R. X. Bian, T. T. Wang, L. Y. Zhang, L. Li and C. G. Wang, *Biomater. Sci.*, 2015, **3**, 1270–1278.

86 L. He, T. T. Wang, J. P. An, X. M. Li, L. Y. Zhang, L. Li, G. Z. Li, X. T. Wu, Z. M. Su and C. G. Wang, *CrystEngComm*, 2014, **16**, 3259–3263.

87 Y. T. Qin, H. Peng, X. W. He, W. Y. Li and Y. K. Zhang, *ACS Appl. Mater. Interfaces*, 2019, **11**, 34268–34281.

88 M. N. He, J. J. Zhou, J. Chen, F. C. Zheng, D. D. Wang, R. H. Shi, Z. Guo, H. B. Wang and Q. W. Chen, *J. Mater. Chem. B*, 2015, **3**, 9033–9042.

89 F. P. Shu, D. J. Lv, X. L. Song, B. Huang, C. Wang, Y. Z. Yu and S. C. Zhao, *RSC Adv.*, 2018, **8**, 6581–6589.

90 P. C. Jiang, Y. L. Hu and G. K. Li, *Talanta*, 2019, **200**, 212–217.

91 Y. Lv, D. D. Ding, Y. X. Zhuang, Y. S. Feng, J. P. Shi, H. W. Zhang, T. L. Zhou, H. M. Chen and R. J. Xie, *ACS Appl. Mater. Interfaces*, 2019, **11**, 1907–1916.

92 H. X. Zhao, G. Shu, J. Y. Zhu, Y. Y. Fu, Z. Gu and D. Y. Yang, *Biomaterials*, 2019, **217**, 119332–119339.

93 Y. C. Ma, Y. H. Zhu, X. F. Tang, L. F. Hang, W. Jiang, M. Li, M. I. Khan, Y. Z. You and Y. C. Wang, *Biomater. Sci.*, 2019, **7**, 2740–2748.

94 Y. T. Li, J. Jin, D. W. Wang, J. W. Lv, K. Hou, Y. L. Liu, C. Y. Chen and Z. Y. Tang, *Nano Res.*, 2018, **11**, 3294–3305.

95 Z. F. Tian, X. X. Yao and Y. F. Zhu, *Microporous Mesoporous Mater.*, 2017, **237**, 160–167.

96 L. H. Su, Q. Wu, L. F. Tan, Z. B. Huang, C. H. Fu, X. L. Ren, N. Xia, Z. Z. Chen, X. Y. Ma, X. D. Lan, Q. Zhang and

X. W. Meng, *ACS Appl. Mater. Interfaces*, 2019, **11**, 10520–10531.

97 H. Y. Zhang, Q. Li, R. L. Liu, X. K. Zhang, Z. H. Li and Y. X. Luan, *Adv. Funct. Mater.*, 2018, **28**, 1802830–1802839.

98 J. C. Yang, Y. Shang, Y. H. Li, Y. Cui and X. B. Yin, *Chem. Sci.*, 2018, **9**, 7210–7217.

99 L. Tang, J. F. Shi, X. L. Wang, S. H. Zhang, H. Wu, H. F. Sun and Z. Y. Jiang, *Nanotechnology*, 2017, **28**, 275601–275629.

100 Z. Zou, S. Q. Li, D. G. He, X. X. He, K. M. Wang, L. L. Li, X. Yang and H. F. Li, *J. Mater. Chem. B*, 2017, **5**, 2126–2132.

101 X. L. Wang, X. L. Li, X. Y. Liang, J. Y. Liang, C. Zhang, J. Yang, C. Wang, D. Kong and H. F. Sun, *J. Mater. Chem. B*, 2018, **6**, 1000–1010.

102 Q. L. Fang, Y. H. Sun, J. Y. Duan, L. F. Bai, K. Z. Xu, Q. S. Xiong, H. J. Xu, K. C. Leung, A. L. Hui and S. H. Xuan, *CrystEngComm*, 2019, **21**, 6935–6944.